

cooled to $-40\text{ }^{\circ}\text{C}$, and photolyzed with Pyrex-filtered light at $-40\text{ }^{\circ}\text{C}$ for 40 min. The ^1H NMR of the resulting mixture (CDCl_3) showed the formation of $\text{Ph}(p\text{-Tol})\text{C}=\text{NPh}$ in 94% yield as well as nitrene complex **7** (δ 3.83, s, 6 H) in 66% yield. Complex **7** was found to persist for several hours in solution. Additional spectroscopic data for **7** (variable-temperature ^1H NMR, ^{13}C NMR, ^{15}N NMR, and IR) are reported and discussed in detail in ref 12. The original spectra for **7** are also available in the supplementary material of ref 12.

Reaction of 7 with Benzaldehyde. Carbene **19** (16 mg, 0.033 mmol) in 0.5 mL of toluene- d_6 was added to triazene **20** (25 mg, 0.17 mmol). The solution was transferred to an NMR tube and photolyzed at $-40\text{ }^{\circ}\text{C}$ with Pyrex-filtered light for 40 min. ^1H NMR of the resulting mixture showed the appearance of **7** (δ 2.77, s, 6 H). An excess of benzaldehyde

(50 mg, 0.47 mmol) was added to this solution, and the mixture was allowed to stand in the dark at room temperature for 13 h. ^1H NMR spectra of the resulting solution showed the disappearance of **7**, and the formation of $\text{PhHC}=\text{NNMe}_2$ (δ 2.65, s, 6 H) in 85% yield.

Acknowledgment. Funding for this work was provided by the Petroleum Research Fund and the NSF-MRL Program through the Center for Materials Research at Stanford University. A.K.C. thanks Undergraduate Research Opportunities, Stanford University for a Major Grant for Extended Research. We thank Claudia Tata Maxey for providing the authentic samples of **9** and **17a**.

Preparation and Spectroscopic Properties of the η^2 -Dihydrogen Complexes $[\text{MH}(\eta^2\text{-H}_2)(\text{PR}_2\text{CH}_2\text{CH}_2\text{PR}_2)_2]^+$ ($\text{M} = \text{Fe}, \text{Ru}$; $\text{R} = \text{Ph}, \text{Et}$) and Trends in Properties down the Iron Group Triad

Maria T. Bautista, E. Paul Cappellani, Samantha D. Drouin, Robert H. Morris,*
Caroline T. Schweitzer, Andrea Sella, and Jeffery Zubkowski

Contribution from the Department of Chemistry and the Scarborough Campus, University of Toronto, Toronto, Ontario M5S 1A1, Canada. Received October 19, 1990

Abstract: Complexes $\text{trans-}[\text{M}(\text{H})(\eta^2\text{-H}_2)\text{L}_2]\text{BF}_4$ ($\text{L} = \text{PPh}_2\text{CH}_2\text{CH}_2\text{PPh}_2 = \text{dppe}$ (**1Fe**, **1Ru**), $\text{PEt}_2\text{CH}_2\text{CH}_2\text{PEt}_2 = \text{depe}$ (**2Ru**)) are prepared by reaction of $\text{cis-}[\text{M}(\text{H})_2\text{L}_2]$ with 1 equiv of $\text{HBF}_4\cdot\text{Et}_2\text{O}$. Deprotonation of **1Ru** by BuLi at 200 K, gives thermally unstable $\text{trans-}[\text{Ru}(\text{H})_2(\text{dppe})_2]$, which isomerizes to $\text{cis-}[\text{Ru}(\text{H})_2(\text{dppe})_2]$. Tetraphenylborate salts of the complexes **1Fe**, **2Fe**, and **2Ru** are prepared by reaction of $\text{trans-}[\text{M}(\text{Cl})(\text{H})\text{L}_2]$ with NaBPh_4 under 1 atm of H_2 . **2Fe**, **1Ru**, and **2Ru** can also be made directly from the complexes $\text{cis-}[\text{MCl}_2\text{L}_2]$ by reaction with 1 atm of H_2 , excess NaBPh_4 , and 1 equiv of NaOEt (or NaO^iBu) in THF. Some properties of the complexes $[\text{Os}(\text{H})(\text{H}_2)(\text{L}_2)]^+$ ($\text{L} = \text{dppe}$ (**1Os**), depe (**2Os**)) are included to reveal trends down the triad of metals; $\text{ReH}_3(\text{dppe})_2$ also provides useful comparisons. The terminal hydride stretching mode, $\nu(\text{M-H})$, increases in frequency as $\text{Fe} < \text{Ru} < \text{Os}$, and the ^{31}P chemical shifts increase in the order $\text{Fe} < \text{Ru} < \text{Os}$ as expected for isostructural complexes. However, indicators of dihydrogen vs dihydride character show that Ru is out of place in the periodic order. ^1H NMR spectra of isotopomers $\text{trans-}[\text{M}(\text{H})(\eta^2\text{-HD})\text{L}_2]^+$ and $\text{trans-}[\text{M}(\text{D})(\eta^2\text{-HD})\text{L}_2]^+$ give couplings $^1J(\text{H,D})$ that decrease as $\text{Ru} > \text{Fe} > \text{Os}$. The chemical shifts of the HD for these two isotopomers are quite different because of the higher trans influence of D than H. The chemical shift difference, $\delta(\text{dihydrogen}) - \delta(\text{terminal hydride})$, for complexes **1** and **2** also decreases as $\text{Ru} > \text{Fe} > \text{Os}$. The T_1 values of the dihydrogen nuclei, $T_1(\text{H}_2)$, and the hydride ligand, $T_1(\text{H})$, were determined over the temperature range of 190–300 K for the complexes **2Fe** and **2Ru** in acetone- d_6 . Analysis of these and other data suggests H–H distances for the rapidly spinning H_2 ligand of the Fe and Ru complexes are comparable at $0.87 \pm 0.02 \text{ \AA}$. An overall ordering of increasing distances is $\text{Ru} \approx \text{Fe} < \text{Os}$. The lability of dihydrogen as judged by the qualitative H_2/D_2 rates of exchange increases as $\text{Os} < \text{Fe} < \text{Ru}$. The equilibrium constant for H_2 binding and hence the strength of the H_2 –metal bond likely increases as $\text{Ru} < \text{Fe} < \text{Os}$. Thus, the Ru complexes have the strongest H–H interaction and weakest metal–dihydrogen interaction. The $[\text{RuHL}_2]^+$ unit is a poorer π -back-bonder than the corresponding complexes of either Fe or Os and forms weaker σ -bonds than Os. Electrochemical and infrared data both indicate that the ease of oxidation of the binding sites for N_2 and Cl^- decreases as $\text{ReH}(\text{dppe})_2 \gg [\text{FeH}(\text{depe})_2]^+ > [\text{FeH}(\text{dppe})_2]^+ > [\text{MH}(\text{depe})_2]^+ > [\text{MH}(\text{dppe})_2]^+$ ($\text{M} = \text{Ru}, \text{Os}$). H atom exchange between H_2 and hydride ligands is monitored by variable-temperature ^1H NMR, and spectra are simulated to give ΔG^\ddagger values that decrease as $\text{Ru} > \text{Fe} > \text{Os}$ and $\text{dppe} > \text{depe}$. This exchange likely proceeds via the homolytic cleavage of the H–H bond.

Introduction

Since the report of the first η^2 -dihydrogen complexes,^{1,2} many transition-metal complexes, both stable^{3–21} and unstable^{18,22,23} at

room temperature, have been identified as containing hydrogen ligands with H–H bonding interactions. This is a study of how

- (1) Kubas, G. J.; Ryan, R. R.; Swanson, B. I.; Vergamini, P. J.; Wasserman, H. J. *J. Am. Chem. Soc.* **1984**, *106*, 451–452.
- (2) Kubas, G. J. *Acc. Chem. Res.* **1988**, *21*, 120–128.
- (3) Kim, Y.; Deng, H.; Meek, D. W.; Wojcicki, A. *J. Am. Chem. Soc.* **1990**, *112*, 2798–2800.
- (4) Van Der Sluys, L. S.; Eckert, J.; Eisenstein, O.; Hall, J. H.; Huffman, J. C.; Jackson, S. A.; Koetzle, T. F.; Kubas, G. J.; Vergamini, P. J.; Caulton, K. G. *J. Am. Chem. Soc.* **1990**, *112*, 4831–4841.
- (5) Amendola, P.; Antoniutti, S.; Albertin, G.; Bordignon, E. *Inorg. Chem.* **1990**, *29*, 318–324.
- (6) Cappellani, E. P.; Maltby, P. A.; Morris, R. H.; Schweitzer, C. T.; Steele, M. R. *Inorg. Chem.* **1989**, *28*, 4437–4438 and references therein.

- (7) Chaudret, B.; Commenges, G.; Jalon, F.; Otero, A. *J. Chem. Soc., Chem. Commun.* **1989**, 210–213 and references therein.
- (8) Johnson, T. J.; Huffman, J. C.; Caulton, K. G.; Jackson, S. A.; Eisenstein, O. *Organometallics* **1989**, *8*, 2073–2074.
- (9) Joshi, A. M.; James, B. R. *J. Chem. Soc., Chem. Commun.* **1989**, 1785–1786 and references therein.
- (10) Ricci, J. S.; Koetzle, T. F.; Bautista, M. T.; Hofstede, T. M.; Morris, R. H.; Sawyer, J. F. *J. Am. Chem. Soc.* **1989**, *111*, 8823–8827.
- (11) Baker, M. V.; Field, L. D.; Young, D. J. *J. Chem. Soc., Chem. Commun.* **1988**, 546–548.
- (12) Bautista, M. T.; Earl, K. A.; Maltby, P. A.; Morris, R. H. *J. Am. Chem. Soc.* **1988**, *110*, 4056–7.
- (13) Bautista, M. T.; Earl, K. A.; Maltby, P. A.; Morris, R. H.; Schweitzer, C. T.; Sella, A. *J. Am. Chem. Soc.* **1988**, *110*, 7031–7036.

the physical and spectroscopic properties of the complexes *trans*- $[M(H)(dppe)_2(\eta^2-H_2)]BF_4$ (*dppe* = $PPh_2CH_2CH_2PPh_2$; *M* = Fe (**1Fe**), Ru (**1Ru**), Os (**1Os**)) and *trans*- $[M(H)(depe)_2(\eta^2-H_2)]BF_4$ (*depe* = $PEt_2CH_2CH_2PEt_2$; **2Fe**, **2Ru**, **2Os**) depend on the nature of the iron group metal and on the diphosphine. Preliminary reports of the discovery of complexes **1Fe** and **1Ru**²⁴ and complexes **26**,^{13,25} as well as some of their NMR properties have already appeared. The X-ray and neutron diffraction studies of single crystals of the BPh_4^- salt of **1Fe** show it to have a symmetrically coordinated η^2-H_2 ligand with a H–H separation of 0.82 (2) Å at 20 K (neutron) and 0.9 (1) Å at 293 K (X-ray).¹⁰ This may be compared to the H–H distance of 0.74 Å in free H_2 and to 0.82 (1) Å (neutron) in $W(CO)_3(H_2)(P(i-Pr)_3)_2$,²⁶ 0.82 (1) Å (neutron) in $Fe(H)_2(H_2)(PEtPh)_3$,⁴ and 0.82 (2) Å (X-ray) in $Fe(C_5H_5)_2(C_5H_5CHMeNMe_2P(i-Pr)_2)(H_2)(Ru)(\mu-H)(\mu-Cl)_2-(Ru)(H)(PPh_3)_2$.²⁷ Thus, there is little variation in H–H distances revealed by diffraction methods so far, apart from a recent study of $[Re(H)_4(H_2)(Cyttop)]^+$ where the dihydrogen distance is 1.08 (5) Å.³ The X-ray diffraction study of the BF_4^- salt of **1Os** revealed that the OsP_4 structural unit is perfectly square planar and consistent with an octahedral *trans*- $[Os(H)(dppe)_2(H_2)]^+$ formulation.²⁸ The osmium-bonded hydrogens were not located accurately. Spectroscopic data indicate that **1Os** has a H–H bond length of about 1.0 Å, which is significantly longer than that of the Fe or Ru complexes.²⁹ Crystals of **2Os** have also been examined by X-ray diffraction, but disorder of the *depe* ligands prevented location of H atoms.³⁰ No distinction could be made between a distorted octahedral geometry expected for *trans*- $[Os(H)(H_2)L_2]^+$ versus a pentagonal bipyramidal geometry expected for $[Os(H)_3L_2]^+$ on the basis of the positions of the phosphorus atoms; a cocrystallized mixture of the two forms probably explains the disorder.³¹

Preliminary results based on $^1J(H,D)$ couplings and T_1 measurements at one temperature indicated that H–H bond length increased and the strength decreased as the M– H_2 interaction increased in the order **1Ru** < **2Ru** < **1Fe** < **2Fe** < **2Os**.²⁵ However,

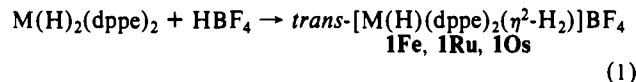
the present work suggests that the Ru and Fe complexes have similar H–H bond lengths. This is a full account of the studies of the iron and ruthenium complexes; the osmium complexes have been described elsewhere,²⁹ but some of their properties are included here to demonstrate the trends in properties down the triad of metals. Comparisons to the properties of the classical trihydride $ReH_3(dppe)_2$ (**3Re**) are illuminating as well.

Other studies of periodic trends have included groups 6, 8, and 9. The stability of the group 6 complexes $M(CO)_3(H_2)(PR_3)_2$ (*R* = *i*-Pr and Cy³²) with respect to loss of the dihydrogen ligand increases as Cr < Mo < W. By contrast, the complexes $M(CO)_5(H_2)$, each with a very labile dihydrogen ligand, increase in stability as Mo < Cr < W; the stretching mode, $\nu(H_2)$, decrease in frequency (Mo > Cr > W) as the stability increases,³³ but this is a consequence of increasing withdrawal of $\sigma(H_2)$ electrons by the metal and to a lesser extent backdonation to $\sigma^*(H_2)$ from the metal. Group 8 dihydrogen complexes exist for Fe and Ru as *mer*- $M(H)_2(H_2)(PR_3)_3$, but the corresponding Os complexes $OsH_4(P(p-tol)_3)_3$ and $OsH_4(PMePh)_3$ have no H–H bonding.¹⁹ Studies of the group 8 series of complexes $[M(H)(H_2)]PPh(OEt)_2$ ₄⁺ revealed that the Os complex might have a longer H–H bond than corresponding Fe and Ru ones on the basis of the longer T_1 time of the dihydrogen ligand.⁵ However, the minimum T_1 values were not observed, and this difference for Os could be due to a more rapid exchange of H atoms between H_2 and hydride sites or due to other factors including differences in rotational correlation times. In keeping with a more hydridic character of the H_2 ligand in the Os complex, it underwent substitution reactions more slowly than the Fe and Ru complexes. The complex $[OsH_3(PPh_3)_4]^+$ is a true trihydride with a nonoctahedral structure.²⁰ Of the group 9 complexes $[MH_2(PP_3)]^+$, the Co complex is an η^2 -dihydrogen complex and the Ir complex is a dihydride, while the Rh complex is thought to have both forms in equilibrium.¹⁵

The study of dihydrogen complexes can assist the understanding of processes like hydrogen storage, hydrogen detection, hydride formation from dihydrogen, and catalytic hydrogenation reactions. Some complexes of η^2 -dihydrogen are precursors to catalysts for the hydrogenation of olefins^{8,9,17,27,34} and the dehydrogenation of alcohols.³⁵ Dihydrogen complexes may also exist in nature; metal centers in hydrogenase and nitrogenase are candidates.^{36,37}

Results

Preparation of the Dihydrogen Complexes. The *dppe* complexes **1** are readily prepared in high yields as the BF_4^- salts by reaction of suspensions in ether of the corresponding dihydride complexes with 1 equiv of $HBF_4 \cdot Et_2O$ (eq 1). Pale yellow (**1Fe**) or white



(**1Ru**, **1Os**)²⁹ precipitates form immediately when the reaction is performed under 1 atm of H_2 . Pure complexes **1Fe** and **1Os** but not **1Ru** are also obtained when an Ar atmosphere is used; solid **1Ru** is only stable under 1 atm of H_2 . A N_2 atmosphere is suitable for the preparation of **1Os**, but not **1Fe** since *trans*- $[Fe(H)(dppe)_2(N_2)]BF_4$ also forms. The complex *trans*- $[Ru(H)(depe)_2(\eta^2-H_2)]BF_4$ has also been prepared by this method from *cis*- $RuH_2(depe)_2$ under 1 atm of Ar.

The complexes prepared from the reaction of $FeH_2(dppe)_2$ and $HClO_4$ ³⁸ or $H_2C(SO_2CF_3)_2$ ^{20,39} are also $[Fe(H)(dppe)_2(H_2)]^+$ salts

(14) Bianchini, C.; Peruzzini, M.; Zanobini, F. *J. Organomet. Chem.* **1988**, *354*, C19–C22.

(15) Bianchini, C.; Mealli, C.; Meli, A.; Peruzzini, M.; Zanobini, F. *J. Am. Chem. Soc.* **1988**, *110*, 8725–8726.

(16) Crabtree, R. H. *Acc. Chem. Res.* **1990**, *23*, 95–101.

(17) Esteruelas, M. A.; Sola, E.; Oro, L. A.; Meyer, O.; Werner, H. *Angew. Chem., Int. Ed. Engl.* **1988**, *27*, 1563–1564.

(18) Gonzalez, A. A.; Mukerjee, S. L.; Chou, S.-J.; Kai, Z.; Hoff, C. D. *J. Am. Chem. Soc.* **1988**, *110*, 4419–4421.

(19) Hamilton, D. G.; Crabtree, R. H. *J. Am. Chem. Soc.* **1988**, *110*, 4126–4133.

(20) Siedle, A. R.; Newmark, R. A.; Korba, G. A.; Pignolet, L. H.; Boyle, P. D. *Inorg. Chem.* **1988**, *27*, 1593–1598.

(21) Mediati, M.; Tachibana, G. N.; Jensen, C. M. *Inorg. Chem.* **1990**, *29*, 3–4.

(22) Chinn, M. S.; Heinekey, D. M.; Payne, N. G.; Sofield, C. D. *Organometallics* **1989**, *8*, 1824–1826 and references therein.

(23) Howdle, S. M.; Poliakov, M. *J. Chem. Soc., Chem. Commun.* **1989**, 1099 and references therein.

(24) Morris, R. H.; Sawyer, J. F.; Shiralian, M.; Zubkowski, J. *J. Am. Chem. Soc.* **1985**, *107*, 5581–2.

(25) Bautista, M.; Earl, K. A.; Morris, R. H.; Sella, A. *J. Am. Chem. Soc.* **1987**, *109*, 3780–2.

(26) Kubas, G. J.; Unkefer, C. J.; Swanson, B. I.; Fukushima, E. *J. Am. Chem. Soc.* **1986**, *108*, 7000–9.

(27) Hampton, C.; Cullen, W. R.; James, B. R. *J. Am. Chem. Soc.* **1988**, *110*, 6918–6919.

(28) Farrar, D. H.; Maltby, P. A.; Morris, R. H. *Acta Crystallogr., Sect. C* **1991**, in press.

(29) Earl, K. A.; Jia, G.; Maltby, P. A.; Morris, R. H. *J. Am. Chem. Soc.* **1991**, *113*, 3027–3039.

(30) Earl, K. A.; Morris, R. H.; Sawyer, J. F. *Acta Crystallogr., Sect. C* **1989**, *C45*, 1137–1139.

(31) Two tautomers of **2Os** are thought to be rapidly interconverting, even at 180 K: an octahedral dihydrogen complex ($[Os(H_2)HL_2]^+$ with an H–H distance of 1 Å as the minor isomer and a trihydride complex ($[Os(H)_3L_2]^+$) with all H–H distances greater than 1.6 Å as the major one. The evidence for this is that the equilibrium is sensitive to changes in the solvent and temperature so that the averaged $J(H,D)$ coupling (ranging from 10.5 to 12.5 Hz) of the $[Os(HD)DL_2]^+$ complex and the averaged chemical shift and minimum T_1 time of the H_2 unit also change. An alternative interpretation cannot be ruled out in which **2Os** is an unusual trihydride with two closely spaced hydrides 1.4–1.5 Å apart. The H–H distance might be sensitive to these changes in conditions.²⁹

(32) Gonzalez, A. A.; Hoff, C. D. *Inorg. Chem.* **1989**, *28*, 4295.

(33) Upmacis, R. K.; Poliakov, M.; Turner, J. J. *J. Am. Chem. Soc.* **1986**, *108*, 3645–3651.

(34) Tsukahara, T.; Kawano, H.; Ishii, Y.; Takahashi, T.; Saburi, M.; Uchida, Y.; Akutagawa, S. *Chem. Lett.* **1988**, 2055–2058.

(35) Morton, D.; Cole-Hamilton, D. J.; Utuk, I. D.; Paneque-Sosa, M.; Lopez-Poveda, M. *J. Chem. Soc., Dalton Trans.* **1989**, 489–495.

(36) Crabtree, R. H. *Inorg. Chim. Acta* **1986**, *125*, L7–L8.

(37) Burrow, T. E.; Lazarowich, N. J.; Morris, R. H.; Lane, J.; Richards, R. L. *Polyhedron* **1989**, *8*, 1701–1704.

(38) Giannoccaro, P.; Rossi, M.; Sacco, A. *Coord. Chem. Rev.* **1972**, *8*, 77–79.

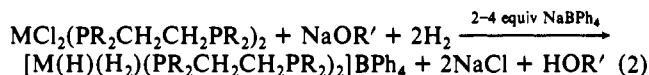
Table I. Hydride Stretching Frequencies (Nujol) and ^{31}P NMR Data (Acetone Solvent; versus H_3PO_4) for the Complexes That Show Periodic Trends

	complex	$\nu(\text{M-H})$, cm^{-1}	$\delta(^{31}\text{P})$
1Fe	$[\text{Fe}(\text{H}_2)(\text{H})(\text{dppe})_2]\text{BF}_4$	1919	92.5
1Ru	$[\text{Ru}(\text{H}_2)(\text{H})(\text{dppe})_2]\text{BF}_4$	1961	68.6
1Os	$[\text{Os}(\text{H}_2)(\text{H})(\text{dppe})_2]\text{BF}_4$	1997	37.5
2Fe	$[\text{Fe}(\text{H}_2)(\text{H})(\text{depe})_2]\text{BPh}_4$	1887	97.9
2Ru	$[\text{Ru}(\text{H}_2)(\text{H})(\text{depe})_2]\text{BPh}_4$	1964	60.8
2Os	$[\text{Os}(\text{H}_2)(\text{H})(\text{depe})_2]\text{BPh}_4$	1983, 1937	41.3

and not the complexes previously reported as $[\text{Fe}(\text{H}_3)(\text{dppe})_2]\text{ClO}_4$ or $[\text{FeH}(\text{dppe})_2][\text{HC}(\text{SO}_2\text{CF}_3)_2]$, respectively. $[\text{FeH}(\text{dppe})_2]^+$, when generated by protonating $\text{FeH}(\text{C}_6\text{H}_4\text{PPhCH}_2\text{CH}_2\text{PPh}_2)(\text{dppe})$, immediately reacts with H_2 to give **1Fe**.

Significantly, the reverse of reaction 1, deprotonation of *trans*- $[\text{Ru}(\text{H})(\text{dppe})_2(\eta^2\text{-H}_2)]^+$ by BuLi at -80°C , gives thermally unstable *trans*- $\text{Ru}(\text{H})_2(\text{dppe})_2$, which isomerizes to *cis*- $\text{Ru}(\text{H})_2(\text{dppe})_2$ at room temperature. The acid-base properties of the other complexes are under investigation.

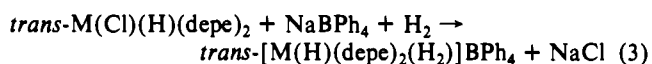
A convenient preparation of the BPh_4^- salts of the complexes **1Ru**, **2Fe**, and **2Ru** involves the reactions of the dichloro complexes with 1 atm of H_2 , excess NaBPh₄, and 1 equiv of NaOEt (or NaO^tBu) in THF/EtOH (eq 2). Only *cis*- $\text{RuCl}_2(\text{depe})_2$ reacts to produce **2Ru**; if some of the unreactive *trans*-dichloro isomer is also present, it is easily separated from the cationic product **2Ru**.



Reaction 2 is thought to proceed via the heterolytic cleavage of dihydrogen in the intermediate complexes $[\text{M}(\text{Cl})(\text{H}_2)(\text{PR}_2\text{CH}_2\text{CH}_2\text{PR}_2)]^+$.⁶ Hydrogen uptake of 1.7 mol/mol Fe occurs in less than 5 min when $\text{FeCl}_2(\text{depe})_2$ in EtOH at 13°C is reacted as in eq 2 to give **2Fe** as a white precipitate. Corresponding preparations of the white ruthenium complexes **1Ru** and **2Ru** take about 4 h at 20°C . The preparation of **1Ru** will proceed without the addition of NaOR' if the reaction flask is continuously purged with H_2 , presumably to remove the HCl that is produced.

The dihydrides $\text{RuH}_2(\text{dppe})_2$, $\text{OsH}_2(\text{dppe})_2$, and $\text{OsH}_2(\text{depe})_2$ can be prepared by a modification of eq 2 where an additional 1 equiv of base (OR⁻) is added to deprotonate the dihydrogen ligand;⁶ a convenient preparation of $\text{RuH}_2(\text{dppe})_2$, which just requires NaOEt, is included in the Experimental Section. $\text{RuH}_2(\text{depe})_2$ has not yet been prepared cleanly by this method. It was prepared by the reaction of $\text{Ru}(\text{cod})(\text{cot})$ with depe and H_2 .

Equation 2 provides a more direct route to the depe complexes **2** than eq 3, the details of which were reported in a brief form previously.²⁵ The procedure for eq 3 was based on the preparation of the analogous dinitrogen complexes *trans*- $[\text{M}(\text{H})(\text{depe})_2(\text{N}_2)]\text{BPh}_4$.⁴⁰ Complex **1Fe** can also be prepared from $\text{FeCl}(\text{H})(\text{dppe})_2$ in this fashion. In reaction 3, the heterolytic cleavage of the M-Cl bond is assisted by the high trans influence of the hydride.



Complex **1Os** and complexes **2** are soluble and stable to loss of H_2 in THF, acetone, or CH_2Cl_2 (for at least 30 min) under Ar at 22°C . Complex **1Fe** is stable under Ar in THF, acetone, and CH_2Cl_2 up to 50°C . Complex **1Ru** must be kept under 1 atm of H_2 in all these solvents.

Spectroscopic Properties. A terminal hydride stretching mode, $\nu(\text{M-H})$, is detected by infrared spectroscopy for the complexes (Table I), but the weak $\nu(\text{H-H})$ absorption is not. The latter, which is expected below 2600 cm^{-1} ,² may be obscured by overtones

(39) Siedle, A. R.; Newmark, R. A.; Pignolet, L. H.; Howells, R. D. *J. Am. Chem. Soc.* **1984**, *106*, 1510-1511.

(40) Bancroft, G. M.; Mays, M. J.; Prater, B.; Stefanini, F. P. *J. Chem. Soc. A* **1970**, 2146-2149.

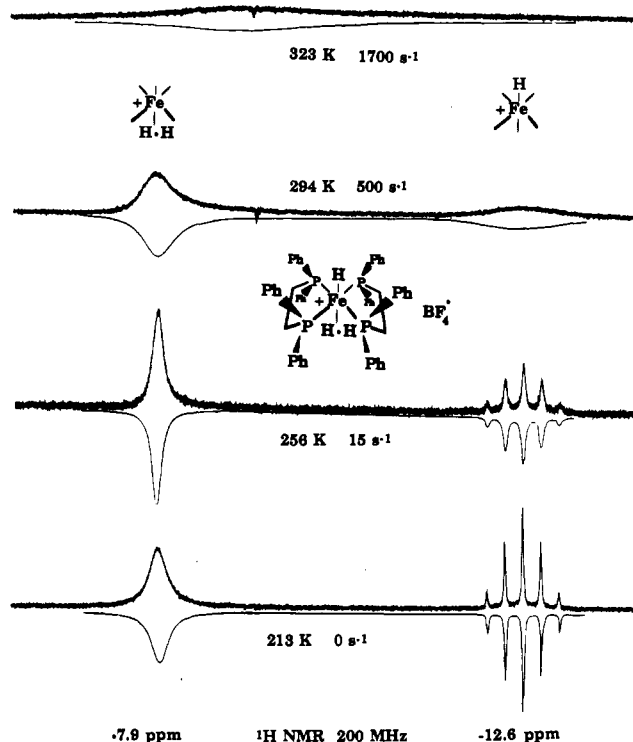


Figure 1. Observed 200-MHz ^1H NMR spectra and simulated (inverted) spectra in the high-field region for the complex $[\text{Fe}(\text{H})(\text{dppe})_2(\text{H}_2)]\text{BF}_4$ (**1Fe**) in acetone- d_6 .

from the ditertiary phosphine ligand vibrations. The $\nu(\text{M-H})$ mode increases in frequency going from Fe to Ru to Os. This trend supports our suggestion that complexes **1** are isostructural η^2 -dihydrogen complexes. Typically the frequency for isostructural neutral complexes increases by $60 \pm 40 \text{ cm}^{-1}$ on going from Fe to Ru and 120 ± 40 from Ru to Os;⁴¹ the order $\nu(\text{Fe-H}) < \nu(\text{Ru-H}) < \nu(\text{Os-H})$ is expected to be maintained in cationic complexes although no infrared studies of this type have been reported yet. The two-band pattern for **2Os** might be due to a cocrystallized mixture of distorted octahedral $(\eta^2\text{-H}_2)(\text{H})$ and pentagonal bipyramidal trihydride tautomers.³¹ A study of inelastic neutron scattering off microcrystalline **1Fe** gave a rotational tunneling splitting of 2.1 cm^{-1} and a barrier to rotational tunneling of $\sim 1.7 \text{ kcal mol}^{-1}$.⁴² In other words, the dihydrogen is rapidly spinning like a propeller in this complex, even in the solid state.

Table I also lists the ^{31}P NMR chemical shift of each complex. For each, the resonance is a singlet that broadens somewhat due primarily to the temperature dependence of T_2 as the temperature is lowered from 300 K to 200 K. The usual periodic trend in $\delta(^{31}\text{P})$ for isostructural phosphine complexes is observed where the chemical shift decreases on going from the 3d to the 4d and then to the 5d metal.⁴³

Low-Temperature ^1H NMR Spectra in the Hydride Region. Complexes **2Fe**²⁵ and **1Os** give temperature-dependent ^1H NMR spectra in the hydride region that are similar to those of **1Fe** shown in Figure 1. The temperature dependence is caused by an intramolecular hydrogen atom exchange process (see below). The spectra for **2Os** differ in that the H_2 chemical shift comes upfield of the terminal hydride in the low-temperature spectra;²⁵ this is further evidence for the existence of two tautomers for this com-

(41) Morris, R. H.; Nassif, O. An unpublished review of metal hydride vibrations reveals these trends for neutral, isostructural complexes MHXL_4 ($\text{L}_2 = \text{dmpe, depe}$; $\text{X} = \text{Cl, Br, I, CN, C}_{10}\text{H}_7$) and $\text{M}(\text{C}_5\text{R}_5)\text{HL}_2$ ($\text{R} = \text{H, Me}$; $\text{M} = \text{Fe, Ru, Os}$; $\text{L} = \text{PPh}_3, \text{PMe}_3$ or $\text{L}_2 = \text{dppe}$).

(42) Eckert, J.; Blank, H.; Bautista, M. T.; Morris, R. H. *Inorg. Chem.* **1989**, *29*, 747-750.

(43) Pregosin, P. S.; Kunz, R. W. *^{31}P and ^{13}C NMR of Transition Metal Phosphine Complexes*; Springer-Verlag: New York, 1979. We find that, for the complexes *trans*- $\text{MHX}(\text{diphosphine})_2$, the following relationships between ^{31}P chemical shifts applies: $\delta(\text{PRu}) \approx 0.81\delta(\text{PFe}) - 6.1$ and $\delta(\text{POs}) \approx 1.04\delta(\text{PRu}) - 34.8$.

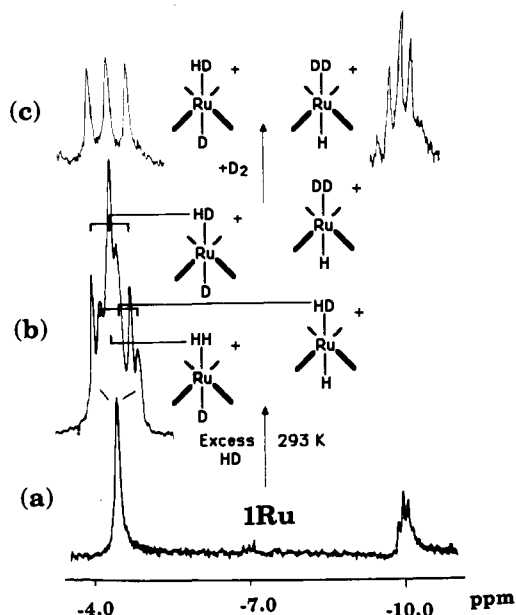


Figure 2. (a) ^1H NMR spectrum at 200 MHz in the high-field region of $[\text{Ru}(\text{H})(\text{dppe})_2(\eta^2\text{-H}_2)]\text{BF}_4$ (**1Ru**) in acetone- d_6 at 293 K, (b) overlapping H_2 and HD resonances produced when **1Ru** is exposed to HD for 5 min, and (c) **1Ru-d** $_2$ isotomers produced by exposing **1Ru** to excess D_2 (300 MHz spectrum).

Table II. ^1H NMR Data at 200 MHz in the Hydride Region for the Complexes in Acetone- d_6 (CD_2Cl_2 for **10s**) and Couplings $^2J(\text{H}, \text{P})$ for the Complexes $\text{trans-}[\text{MH}(\text{diphosphine})_2(\text{CO})]^+$ ($\text{M} = \text{Fe},^a \text{Ru},^{40,85}$ and Os) 29

complex	T, K	$\delta(\text{M-H})$	$^2J(\text{H}, \text{P})$	$\delta(\text{H}_2)$	$^2J(\text{H}_2, \text{P})$	$^2J(\text{H}, \text{P})^b$
1Fe	323	-9.5	nr^c	-9.5	nr^c	
	210	-12.6	-47	-7.9	-5 ± 5	-47
1Ru	293	-10.0	-18	-4.6	0 ± 2	-19.5
1Os	210	-9.0 ^d	-17	-6.8 ^e	-5 ± 2	-19.2
2Fe	290	-11.9	nr^c	-11.9	nr^c	
	220	-14.6	-47.0	-10.5	-1.8	-47
2Ru	293	-11.3	-19.3	-6.4	0 ± 2	-20
	220	-9.7	-17.5	-10.0 ^f	-5.5	-20.4

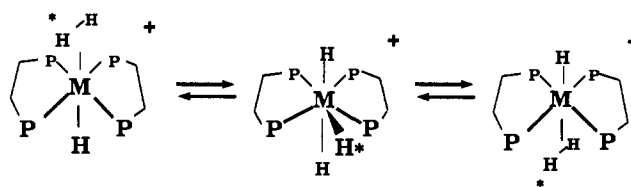
^aThis work, ref 40. ^bValues for the corresponding complex $\text{trans-}[\text{MH}(\text{diphosphine})_2(\text{CO})]^+$. ^cNot resolved, broad singlet. ^dTemperature dependent: $\delta(\text{M-H}) = 0.0056T - 10.20$. ^eTemperature dependent: $\delta(\text{H}_2) = -0.0014T - 6.49$. ^f17 Hz in ethanol- d_6 .¹¹ ^gTemperature dependent: $\delta(\text{H}_2) = 0.0029T - 10.61$.

plex.³¹ The spectra for **1Ru** (see Figure 2) and **2Ru** do not change as the temperature is lowered below 293 K apart from a broadening of the H_2 resonance. The spectra are consistent with the $\text{trans-}[\text{M}(\text{H})(\text{H}_2)(\text{PR}_2\text{CH}_2\text{CH}_2\text{PR}_2)_2]^+$ formulation.

At 210 K and 200 MHz, the terminal hydride resonance of each complex **1** and **2** is a well-resolved, binomial quintet, with the magnitude of the $^2J(\text{H}, \text{P})$ constants typical of couplings between cis ^1H and ^{31}P nuclei in bonds at 90° angles for the respective metal in oxidation state II (see Table II; cf. the $^2J(\text{H}, \text{P})$ values for the analogous carbonyl complexes). Recent work verifies the negative sign of this coupling constant.^{44,45}

The broad dihydrogen resonance at 210 K is found downfield of the quintet except for **2Os**. The Ru complexes, with the weakest interaction with the H_2 ligand, give the lowest field H_2 resonances here and in other complexes,⁴⁶ perhaps because they have the closest properties to free H_2 , which resonates at 4.5 ppm. Another possible indicator of molecular H_2 character is the amount that the chemical shift of the dihydrogen differs from that of the

Scheme I. Intramolecular Exchange of H Atoms between Hydride and Dihydrogen ($\Delta G^\ddagger = 12\text{--}17 \text{ kcal mol}^{-1}$)



hydride in the same molecule, $\delta(\text{dihydrogen}) - \delta(\text{terminal hydride})$. This quantity decreases in the expected order **1Ru** > **2Ru** > **1Fe** > **2Fe** > **1Os** > **2Os** (refer to chemical shifts from low-temperature spectra in Table II). The reversal in positions of the H_2 and H resonances for **2Os** is explained by the fact that the trihydride tautomer predominates.³¹

The large line width of the dihydrogen resonance is explained by the rapid dipolar relaxation of these nuclei plus unresolved $^2J(\text{H}, \text{P})$ couplings (Table II gives estimates of these). Exchange of H atoms between H_2 and terminal hydride ligands is negligible below 220 K for these complexes (see below) and does not contribute to the broadening. A previous study of T_1 and T_2 of some of these complexes could not satisfactorily explain why the lines were so broad for **1Fe** and **2Os**. Explaining this effect as a slowing of the rotation of the $\eta^2\text{-H}_2$ ligand^{14,20,24} is probably not correct since the rate of rotation is many orders of magnitude greater than the possible difference in resonance frequencies of the ^1H nuclei.¹³ The pronounced broadening of the $\eta^2\text{-H}_2$ resonance and the broadening of the hydride resonance as the temperature is lowered below 220 K is explained mainly by the expected decrease in T_2 of the nuclei.

Temperature-Dependent ^1H NMR Spectra Due to the Intramolecular Exchange of H Atoms between η^2 -Dihydrogen and Terminal Hydride Ligands. The fluxional process that explains the spectra of complexes **1Fe** (Figure 1), **2Fe**,²⁵ **1Os**, and **2Os** is an intramolecular exchange of hydrogen atoms between the η^2 -dihydrogen and terminal hydride ligands (Scheme I).

The spectra can be simulated where two equivalent protons, A_2 , in an A_2X_4 spin system with short T_2 values interchange with one proton, B, in a BX_4 spin system with a long T_2 value. J_{AB} is assumed to be negligible. This is valid since none of the complexes can have a J_{AB} ($^2J(\text{H}, \text{H}_2)$) coupling constant that exceeds 3 Hz due to the lack of resolvable additional coupling in the quintet of the terminal hydride. The simulation of the spectra of **1Os** and **2Os** has been described recently, and only the chemical shifts, coupling constants, and activation energies are included here (Tables II and IV). J_{BX} values ($^2J(\text{H}, \text{P})$) are obtained from the quintet at low temperature (see Table II). However, J_{AX} values ($^2J(\text{H}_2, \text{P})$) are obtained indirectly from band shape analysis since they are not resolved in the broad H_2 resonance at low temperatures. There is a large error in these values because most of the broadening of the H_2 resonance is due to the short T_2 (Table III) and not due to the unresolved quintet structure. Complex **2Fe** in acetone- d_6 gives a broad peak at -11.9 ppm at 293 K or above; however, in ethanol- d_6 , it is reported to give a quintet in spectra at 293 K with a coupling $|J(\text{H}, \text{P})|$ of 17 Hz, which results from the averaging (1:2) of the terminal hydride coupling J_{BX} of -47 Hz with a J_{AX} coupling of -1.8 Hz.¹¹ It is assumed in this calculation that J_{AX} and J_{BX} are temperature invariant. A less accurate J_{AX} value of 5 Hz was previously reported for **2Fe** in acetone- d_6 by spectral simulation.²⁵ Complex **2Os** is a similar case. The J_{AX} couplings must be negative to average correctly with the negative J_{BX} couplings to produce the averaged $J(\text{H}, \text{P})$ coupling in the fast exchange spectrum.^{44,45} Broad singlets instead of quintets are observed in the fast exchange spectra of **1Fe** and **1Os** up to 330 K so that J_{AX} values of Table II for these complexes are rough estimates from the simulation of the line widths. It should be noted that no coupling $^2J(\text{H}, \text{P})$ is resolved in the sharp ^1H NMR resonance (1:1:1 triplet) of the HD ligand of the deuterated complexes **1**, **2Fe**, and **2Ru** (see below) so that the $^2J(\text{H}_2, \text{P})$ couplings of Table II can be considered as maximum possible values. Such couplings to the HD ligand have been resolved for

(44) Benn, R.; Jousen, E.; Lehmkuhl, H.; López Ortiz, F.; Rufinska, A. *J. Am. Chem. Soc.* **1989**, *111*, 8754-8756.

(45) Eisenschmid, T. C.; McDonald, J.; Eisenberg, R.; Lawler, R. G. *J. Am. Chem. Soc.* **1989**, *111*, 7267-7269 and references therein.

(46) Antoniutti, S.; Albertin, G.; Amendola, P.; Bordignon, E. *J. Chem. Soc., Chem. Commun.* **1989**, 229-230.

Table III. T_2 Values and Rates of H Atom Exchange (k) from the Dihydrogen (H_2) Sites to the Terminal Hydride (H) Site Obtained by Line Shape Analysis and T_1 Values Measured by the Inversion Recovery Method^a

complex	T , K	$T_2(H_2)$, ms	$T_1(H_2)$, ms	$T_2^*(H)$, ms	$T_1^*(H)$, ms	k , s ⁻¹	
1Fe^b	329	56 (56)		570 (570)		2300	
	323	53 (53)		530 (528)		1700	
	294	25 (25)	40* (40*)	350 (350)	40* (40*)	500	
	256	13 (13)		188 (190)		15	
	224	7.0 (7.0)	10 (9)	100	130 (131)	7	
	213	6	9 (8.5)	80 (83)	130	0	
1Ru^b	285	11* (25)	29* (27*)		294* (357)	2	
2Fe^b	322	134 (134)		298* (3070)		9000	
	294	87 (87)		252* (1990)		1374	
	276	63 (63)		220* (1445)		330	
	257	25 (25)		190* (980)		58	
	238	20 (20)		160* (630)		7.8	
	219	15 (16)		130 (370)		0.7	
	210	12 (13)	12	120 (290)	302	0.2	
	200	10 (9)		100 (210)		0.03	
	2Fe^c	270		98* (84*)		107* (84*)	
		230		31* (31*)		145* (31*)	
213			31 (19)		391 (428)		
211			17 (17)		415 (410)		
190		7 (9)	16 (17)		378 (393)		
180			19 (20)		355 (462)		
210			11		270	0	
2Ru^b	295		70 (83)		241* (2132)	10	
	273		56 (57)		895* (1457)	1	
	253		40 (39)				
	232		26 (25)				
	212		18 (18)		502 (461)		
	193		16 (16)		403 (401)		
	183		20 (17)		424 (445)		

^a For T_1 data for **1Fe**, **1Ru**, **1Os**, and **2Os**, see also refs 13 and 29. Values in parentheses were calculated from temperature-dependent T_1 and T_2 equations as described in refs 13 and 48 by use of the parameters listed in Tables IV and V. The values with asterisks indicate that they are averaged due to the H atom exchange process. ^b 200 MHz, acetone- d_6 . ^c 400 MHz, acetone- d_6 .

$[Ru(Cp)(dmpe)(HD)]^{+47}$ and $[OsD(depe)_2(HD)]^{+29}$

The chemical shifts of the fast exchange spectra of complexes **1Fe** and **2Fe** are weighted averages (2:1) of $\delta(H_2)$ and $\delta(H-M)$. This is not true of the osmium analogues unless temperature dependences of the chemical shifts of the η^2-H_2 and H ligands are accounted for (Table II).

Spectra calculated on the basis of this information match observed spectra very well (see Figure 1, refs 25, 29). The rate constant, k , for H atoms going from the dihydrogen sites to the terminal hydride site (the rate constant for the reverse process would be $2k$) and T_2 values from the simulations are listed in Table III. For complex **1Fe** in acetone- d_6 , the T_2 values match those calculated with use of the temperature dependence of the correlation time from the T_1 measurements in the T_2 equation; the agreement was not as good for data obtained at 200 MHz with **1Fe** in CD_2Cl_2 .¹³ For **2Fe**, the T_2 values of the terminal hydride from the simulations are shorter than the ones calculated. Eyring plots of $\ln(k/T)$ vs $1/T$ are linear, and from them the activation parameters listed in Table IV are derived.

At room temperature, the fluxional process of Scheme I is slow for complexes **1Ru** and **2Ru** but is detected by spin saturation transfer experiments and averaging of the T_1 values of the H_2 and hydride ligands (rate for **1Ru** at 285 K is given in Table III). An estimate of ΔG^\ddagger for this process for **1Ru** is given in Table IV. Above room temperature, intermolecular exchange of the ruthenium complexes with free $H_2(g)$ dominates as indicated by continuous broadening of the peaks as the temperature is raised; thus, the observation of spectra characteristic of fast intramolecular exchange is not possible.

Longitudinal Relaxation Times, T_1 , of the H_2 and H Ligands. The T_1 values of the dihydrogen nuclei, $T_1(H_2)$, and the hydride ligand, $T_1(H)$, were determined over the temperature range of 190–300 K for the complexes in acetone- d_6 (Table III). When the rate of intermolecular H atom exchange exceeds about 10 s^{-1} (Table III), then the rates of relaxation ($1/T_1$) of the H_2 and

Table IV. Activation Parameters (kcal mol⁻¹) from the Eyring Equation for the Intramolecular Exchange of H Atoms between η^2-H_2 and Terminal H Sites and between cis and trans Isomers of Related Dihydride Complexes^a

complex	ΔH^\ddagger	ΔS^\ddagger	ΔG^\ddagger (300 K)
1Fe	11.0	-10.0	14.0 ± 0.3
1Ru			15.6 ± 0.5 ^b
1Os	9.9	-11.5	13.3 ± 0.3
3Re			12.7 ± 0.5
2Fe	12.2	-2.5	13.0 ± 0.2
2Ru			>15
2Os	9.1	-12.9	12.9 ± 0.2
FeH ₂ (dppe) ₂			14.3 ³⁴
RuH ₂ (dppe) ₂			19.3 ³⁴
OsH ₂ (dppe) ₂			>20
FeH ₂ (dmpe) ₂ ^c			16.2 ³⁴

^a The values for **1Os**, **2Os**, and **3Re** are from ref 29. ^b Estimated from the rate of T_1 averaging. ^c dmpe = $PMe_2CH_2CH_2PMe_2$.

hydride nuclei start to average. Above exchange rates of about 100 s^{-1} , the observed relaxation rates are averages of the H_2 and hydride rates weighted 2:1.

The analysis of some of this data to obtain the H–H distance, r_{HH} , of the complexes **1Fe** and **1Ru**¹³ and **1Os** and **2Os**²⁹ has already been described. The calculations involve fitting the equations that describe the spin lattice relaxation by the dipolar mechanism⁴⁸ to the temperature dependent T_1 data by use of a computer program that varies r_{HH} , τ_0 (reflecting the size of the molecule), and E_a (a measure of the viscosity of the solvent).¹³ It is important to use a spectral density function that takes into account the spinning of the dihydrogen, which is a much higher frequency process than the tumbling of the molecule.¹³ The best fit pa-

(48) The equation for dipolar relaxation is $1/T_1 = 0.3\gamma_H^4(h/2\pi)^2(J(\omega) + 4J(2\omega))/r_{HH}^6$. The spectral density function is given by $J(\omega) = A\tau/(1 + \omega^2\tau^2)$ where $A = 0.25$ for rapid rotation of the H_2 ligand or $A = 1.0$ for no rotation of the H_2 . The temperature dependence of the correlation time is assumed to be $\tau = \tau_0 e^{E_a/RT}$. At the temperature of minimum T_1 , $\tau = 0.62/(2\pi\nu)$ and these equations simplify to $r_{HH} = 4.611(T_1(\text{min})/\nu)^{1/6}$ for rapid rotation and $r_{HH} = 5.815(T_1(\text{min})/\nu)^{1/6}$ for no rotation (ν (MHz), T_1 (s)).

(47) Chinn, M. S.; Heinekey, D. M. *J. Am. Chem. Soc.* **1987**, *109*, 5865–5867.

Table V. Minimum T_1 value ($T_1(\text{min})$) for the Dihydrogen Ligand (at Temperature, $T(\text{min})$ and Spectrometer Frequency ν) Obtained by Direct Observation and/or Fitting the Data of Table III to the Temperature-Dependent T_1 Equation by Using a Temperature-Dependent Correlation Time $\tau = \tau_0 e^{E_a/RT}$.¹³

complex	ν , MHz	$T(\text{min})$, K	$T_1(\text{min})$, ms	τ_0 , ps	E_a , kcal mol ⁻¹	r_{H_2} , Å	
						min ^b	max ^c
1Fe	200	207	8.5 ± 1	0.90	2.6	0.86	0.87
	400	230	17 ± 1	0.90	2.6	0.86	0.87
1Ru	200	205	10 ± 1	1.08	2.5	0.88	0.90
	400	230	20 ± 1	1.08	2.5	0.88	0.90
1Os	200	205	18 ± 1	0.90	2.6	0.98 ^c	1.02 ^d
	400	233	40 ± 1	0.90	2.6	0.99 ^c	1.02 ^d
2Fe	400	180	16 ± 1	0.17	2.9	0.85	0.86
2Ru	400	195	16 ± 1	0.18	2.8	0.85	0.86
2Os	400	203	80 ± 2	0.19	2.9	(1.12) ^e	(1.17) ^e

^a The H-H distance of the dihydrogen ligand r_{H_2} is calculated for the case of rapid rotation of the dihydrogen with respect to the tumbling of the molecule. CD₂Cl₂ solvent of **1Os**, acetone-*d*₆ for the others. ^b Obtained by fitting T_1 data to relaxation equations for rapid rotation of the H₂ ligand.⁴⁸ ^c Calculated by use of $T_1(\text{H}_2, \text{true})$ value as in eq 4. ^d The possibility of a high barrier to H₂ rotation has not been completely ruled out for **1Os**. If this were the case, then the H-H distance from a nonspinning H₂ unit would be about 1.3 Å. ^e This value is not correct because it results from the averaging of properties of two tautomers.³¹

parameters for all the complexes are found in Table V.

The distances r_{H_2} obtained from the fit are listed as minimum distances in Table V. The distances will actually be slightly longer than these (r_{H_2} maximum) because of dipolar interactions of the H₂ nuclei with other nuclei with spins in the molecule (see below). The distances were calculated assuming rapid spinning of the H₂ ligand ($A = 0.25^{48}$). This is a good assumption for the complexes **2Fe**, **1Ru**, and **2Ru** based on their similarity to **1Fe**, which is known to have a rapidly spinning H₂, even in the solid state. If the correlation time of the H₂ were not shorter than the one for the tumbling of the molecule (i.e., no H₂ spinning), then the H-H distance could fall in a second range of distances (1.10–1.14 Å) ($A = 1.0^{48}$); the observation of large $^1J(\text{H},\text{D})$ values for these complexes (ca. 30–33 Hz) makes this an unlikely situation. Distances in the range 0.9–1.1 Å can be ruled out since they would arise from intermediate rotation rates that give plots of $\ln T_1$ versus $1/T$ with curves characteristically different to those observed (see Figure 4 of ref 13). No fit to the data could be obtained by use of an intermediate H-H distance of around 1 Å and by letting E_a and τ_0 vary. The octahedral complex **1Os** should also have a spinning H₂, but this needs to be verified by inelastic neutron scattering. A longer H-H distance of 1.25 Å would be expected for **1Os** without H₂ spinning, but this is not consistent with the large $^1J(\text{H},\text{D})$ value observed for the HD complex. The assumption of rapid spinning is not valid for complex **2Os**, which consists mainly of a trihydride with a nonspinning H₂ unit so that the H-H distance reported in Table V is an averaged one with little physical significance.³¹

The τ_0 and E_a parameters obtained by the fitting procedure describe fairly successfully the temperature dependence of the T_1 values of the terminal hydride (Table VI) as well as the H₂ nuclei (Table V). The τ_0 values are smaller for the smaller depe complexes **2** than the dppe ones. Complexes with the same ligand have similar τ_0 values; experimental uncertainties do not allow a definitive ranking of the sizes of the Fe, Ru, and Os complexes based on τ_0 .

Minimum $T_1(\text{H}_2)$ values were directly observed in either the 200- or 400-MHz series of measurements apart from **1Fe**, where the intramolecular H atom process masked the minimum at both frequencies. However, a minimum value is readily obtained from the fitted T_1 curve for this complex.¹³ The smaller complexes **2** go through the minimum at a low temperature, $T(\text{min})$, of about 189 K at 200 MHz or 200 K at 400 MHz, whereas the larger complexes **1** have higher $T(\text{min})$ of 205 K at 200 MHz and 230 K at 400 MHz. The same dihydrogen bond distance r_{H_2} (Table V, minimum value) is obtained from the fit to the data or from the $T_1(\text{min})$ value (when it is observed) according to the procedure of Hamilton and Crabtree.^{19,48}

The true H-H distances are likely to be a little longer than $r_{H_2}(\text{min})$ of Table V because other protons on the dppe ligands contribute to the relaxation of the H₂ nuclei as do the phosphorus nuclei and possibly the metal (see below). The major contributor will be hydrogens on the ligands because phosphorus and the

Table VI. Observed Minimum T_1 Value ($T_1(\text{min})$) for the Terminal Hydride Ligand Obtained by Direct Observation and Fitting to the Temperature-Dependent T_1 Equation (Same $T(\text{min})$, τ_0 , E_a as Corresponding Complex Entry in Table V)^a

complex	ν , MHz	$T_1(\text{min})$, s	¹ H NMR		³¹ P NMR	
			r_{H-H} , Å	$T_1(\text{min})$, s	$T_1(\text{min})$, K	$T_1(\text{min})$, s
1Fe	200	0.12	1.7	2.1	192	0.24
	400	0.24	1.7	2.1		
1Ru	200	0.14	1.7	2.2	196	0.37
	400	0.27	1.7	2.2		
1Os	400	0.28	1.7	2.2	200	0.52
2Fe	400	0.38	1.8	2.3		
2Ru	400	0.4	1.8	2.3		
2Os	200	0.17	1.8	2.2		
	400	0.34	1.8	2.2		

^a The T_1 values for the phosphorus nuclei (determined at 162 MHz) are also included. ^b $r_{H-H} = 5.815 (T_1(\text{min})/\nu)^{1/6}$ with r in angstroms, T_1 in seconds, and ν , the spectrometer frequency, in megahertz.⁴⁸ ^c Multiply minimum distance by $4^{1/6}$ to account for four nearby protons.

metals have much smaller magnetogyric ratios, γ_X , than hydrogen, γ_H , and heteronuclear dipolar relaxation depends on γ_H^2/γ_X^2 . Also the P nuclei are farther away (≥ 2.6 Å) from the H₂ nuclei than are ligand hydrogens (2.0–2.2 Å). The contribution from these other sources of relaxation can be approximated by use of the observed minimum T_1 value of the terminal hydride, $T_1(\text{H}, \text{obs})$, since this hydride is in a similar environment to the H₂ ligand (eq 4).⁴⁹ As an example, complex **1Ru** has minimum values of

$$\frac{1}{T_1(\text{H}_2, \text{obs})} = \frac{1}{T_1(\text{H}_2, \text{true})} + \frac{1}{T_1(\text{H}, \text{obs})} \quad (4)$$

$T_1(\text{H}_2, \text{obs}) = 0.020$ and $T_1(\text{H}, \text{obs}) = 0.27$ s at 400 MHz (Tables V and VI). The former value corresponds to an r_{H_2} of 0.88 Å. The corrected minimum $T_1(\text{H}_2, \text{true})$ is 0.022 s, and the corrected maximum H-H distance is 0.90 Å, assuming rapid spinning. Note that the dihydrogen H-H distances for the Fe and Ru complexes are only slightly lengthened when the correction via eq 4 is applied (Table V), whereas there is a greater lengthening of the Os H-H distances.

From the minimum T_1 values for the terminal hydride resonances, one can estimate the distance (r_{H-H}) to protons on the ligands that cause it to relax. The distances given in ref 13 were calculated on the assumption that only one ligand proton comes close to the terminal hydride at a given time; this proton is likely to be a phenyl ortho proton for dppe or a methyl proton for depe.

(49) The dihydrogen protons, while they are spinning, could approach closer (by about 0.2 Å) than a terminal hydride to an ortho hydrogen on a dppe ligand or a hydrogen on a methyl of a depe ligand; however, the distance from the centroid of rotation of H₂ or from the terminal hydride to the ligand protons should be the same.

Table VII. ^1H NMR Chemical Shifts of Some of the Isotopomers of the Complexes^a

	<i>T</i>	$(\text{H}_2)\text{-M-H}$		$(\text{HD})\text{-M-H}$		$(\text{H}_2)\text{-M-D}$		$(\text{HD})\text{-M-D}$	
		$\delta(\text{H}_2)$	$\delta(\text{HD})$	$^1J(\text{H,D})$	$^2J(\text{H,P})$ for HD	$\delta(\text{H}_2)$	$\delta(\text{HD})$	$^1J(\text{H,D})$	$^2J(\text{H,P})$ for HD
1Fe ^b	210	-8.62	-8.62	30 ± 2	<5	-8.55	-8.56	31.5 ± 1.0 ^d	<5
1Ru	293	-4.57	-4.57	32.0 ± 0.5	<2	-4.50	-4.50	32.8 ± 0.5	<2
1Os	230	<i>c</i>	-6.62	25.5 ± 0.5	<5	-6.61			
2Fe	200	-10.5					-10.5	29.5 ± 0.5	<5
2Ru	293	-6.48	-6.50	32.3 ± 0.5	<2	-6.42	-6.47	31.8 ± 0.5	<2
2Os ^d	200	-10.03	-10.10 ^e	≤10 ^f	-5	-9.93 ^g	-10.02 ^h	10.5 ± 0.1	-5.4

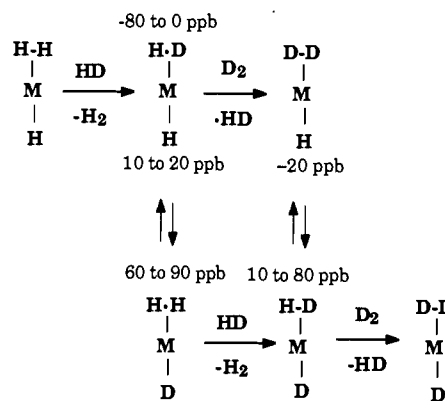
^a 200 MHz, acetone-*d*₆ unless otherwise noted. The terminal hydride chemical shifts for the isotopomers *trans*-[M(H)(HD)L₂]⁺ and *trans*-[M(H)(D)₂L₂]⁺ are within 0.02 ppm of the chemical shift $\delta(\text{H})$ for *trans*-M(H)(H₂) (see Scheme II). ^b CD₂Cl₂. ^c -6.80 in CD₂Cl₂. ^d 400 MHz. ^e $\delta(\text{HD}) = 0.0031T - 10.65$. ^f From line shape analysis. ^g $\delta(\text{H}_2) = 0.0028T - 10.49$. ^h $\delta(\text{HD}) = 0.0034T - 10.70$.

A maximum of about four ligand protons at equal distance to the hydride could cause its relaxation; then that distance can be longer than the previous case by a factor of $4^{1/6} = 1.26$; these $r_{\text{H-H}}$ distances are indicated in Table VI as maximum values. For the sake of comparison, hydride to ortho hydrogen distances for **1Fe** of 1.9–2.2 Å were measured on a model built from the dimensions of the neutron diffraction structure. Similar distances were measured on a scale model of a similar osmium complex with 2.36-Å Os–P distances and a 1.7-Å Os–H distance. The range of distances of 1.7–2.3 Å calculated on the basis of the T_1 values is not unreasonable (Table VI). When the ligand protons are replaced by deuteria, the relaxation time for the terminal hydride of **1Fe** or **1Os** dramatically increases whereas the T_1 of the H₂ ligand is unaffected; this should be the case when the hydrogens ortho on the phenyls are the main contributors to the relaxation rate of the terminal hydride (deuterium, with its small γ_{D} value, is a less efficient dipolar relaxation agent), whereas the hydrogens in the H₂ ligand are solely responsible for each other's relaxation rate.¹³

The long comparable T_1 value for the terminal hydride in each of the complexes supports the idea that relaxation of the nuclei is due to dipolar interactions and not due to paramagnetic impurities or other modes of relaxation. To examine this, we also determined the minimum T_1 value of the phosphorus nuclei in complexes **1** (Table VI). These values do parallel approximately the minimum T_1 values in Table VI of the hydride. The approach of correcting the $T_1(\text{H}_2, \text{obs})$ value with the terminal hydride's relaxation rate (eq 4) should account for these differences in relaxation due to the metal and other nuclei at varying distances from the dihydrogen nuclei in the molecule.

H₂/D₂ Exchange. A qualitative rate of hydrogen loss was obtained by shaking solutions of the complexes **2** in acetone-*d*₆ under D₂ at 1 atm and 295 K. The intensity of ^1H NMR resonances in the hydride region drops to half the initial value as **2Ru** (<5 min) < **2Fe** (~2 h) < **2Os** (180 h). The rate of the reaction of D₂ with **2Fe** was independent of the D₂ pressure. Complexes **1** with the dppe ligand are noticeably more labile than their depe counterparts. Complex **1Ru** is so labile that it loses up to 1 mol of H₂ in the solid state at 25 °C under vacuum in 10 min to give orange-yellow [RuH(dppe)₂]BF₄. Hydrogen re-adds in seconds to this five-coordinate complex in the solid state or to [RuH(acetone)(dppe)₂]BF₄, $\nu(\text{CO}) = 1673 \text{ cm}^{-1}$, in acetone solution to give **1Ru**.

Preparation and Properties of the Deuterated Complexes. A variety of isotopomers can be observed by ^1H NMR as the Fe and Ru complexes in acetone-*d*₆ are progressively enriched in deuterium by exposure first to excess HD (prepared from NaH and D₂O) and then to D₂ gas (Figure 2). They are observed when intramolecular H atom exchange is slow (290 K for **1Ru**, **2Ru**; 210 K for **1Fe**, **2Fe**). The isotopomer first formed upon intermolecular exchange of H₂ with HD would be *trans*-[M(H)(HD)L₂]⁺ (Scheme II). However, the isotopomer *trans*-[M(H)(HD)L₂]⁺ also is formed quickly by intramolecular exchange of H atoms. The d₁ complexes can also be prepared by adding HBF₄ in D₂O to the dihydride complex (as in eq 1). The complex **1Fe-d₂** has been prepared by adding HBF₄ to FeD₂(dppe)₂ in ether. The Ru complexes are sometimes enriched in deuterium by slow exchange with acetone-*d*₆; an impurity may be involved in this reaction.

Scheme II. Successive Formation of Isotopomers of Complexes **1** and **2** as They Become Enriched in Deuterium^a

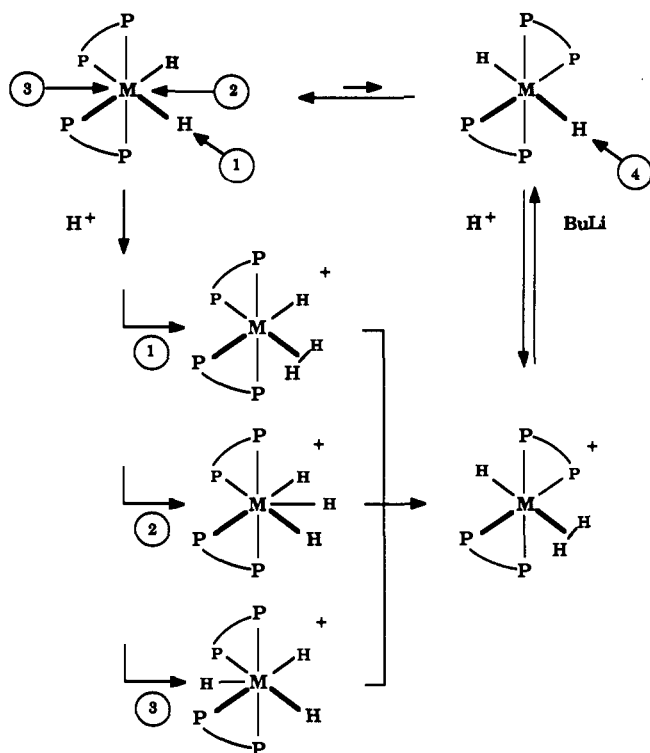
^a The isotope shifts (in parts per billion) refer to the chemical shift of the ^1H in the isotopomer minus the shift of the corresponding resonance in the nondeuterated form of the complex (refer to Table VII).

Table VIII. Selected Electrochemical and Infrared Properties of the Complexes *trans*-[M(H)(diphosphine)₂(L)]⁺

complex	electrochemistry ^a		infrared ^b	
	L = H ₂ , <i>E</i> _a , ^c V	L = Cl ⁻ , <i>E</i> _{1/2} , ^d V	L = CO, $\nu(\text{CO})$, cm ⁻¹	L = N ₂ , $\nu(\text{N}_2)$, cm ⁻¹
[Fe(H)(dppe) ₂ (L)] ⁺	0.8 ^e	-0.71	1950	2120
[Ru(H)(dppe) ₂ (L)] ⁺	>1 ^e	-0.12	1987 ^f	2194
[Os(H)(dppe) ₂ (L)] ⁺	1.15 ^g	-0.14 ^g	2003 ^e	
[Fe(H)(depe) ₂ (L)] ⁺	0.6	-0.98 ^h	1929 ^f	2090 ⁱ
[Ru(H)(depe) ₂ (L)] ⁺	1.1	(-0.24) ^j	1958 ^f	2163 ⁱ
[Os(H)(depe) ₂ (L)] ⁺	1.0 ^e	-0.46 ^{g,k}	1974 ^f	2136 ⁱ
Re(H)(dppe) ₂ (L)	-0.4 ^l (3Re)	-	1845 ^m	2006 ^m

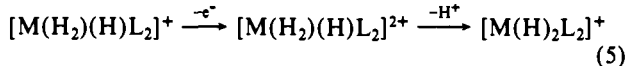
^a Versus FeCp₂/FeCp₂⁺, THF solvent, 0.2 M *n*-Bu₄NBF₄, 200 mV s⁻¹ scan rate unless otherwise noted. ^b Nujol mull unless otherwise noted; this work unless otherwise noted. ^c Anodic peak potential of irreversible wave; complexes **2** are BPh₄⁻ salts and give *E*_a = 0.6 V for BPh₄⁻/BPh₄ oxidation. ^d Values in parentheses are anodic peak potentials. ^e CH₂Cl₂ solvent. ^f Reference 85. ^g 0.2 M *n*-Bu₄NPF₆, 250 mV s⁻¹ scan rate. ^h *E*_a at 0.50 V also; also cathodic peaks at *E*_c = -1.06 and -0.26 V. ⁱ Reference 40. ^j *E*_a at -0.06 and 0.22 V also; *E*_c at -0.37, -0.17, and 0.10 V. ^k *E*_{1/2} at 0.45 V also. ^l 0.19 V versus Ag/AgCl.⁸⁶ ^m Reference 87.

Couplings $^1J(\text{H,D}) \approx 30\text{--}32 \text{ Hz}$ for the Fe complexes and 32–33 Hz for the Ru complexes can be resolved in the ^1H NMR spectra at 210 K for Fe and 293 K for Ru (Table VII) and verify the presence of an H–H bond. There is no resolvable isotopic shift $\delta(\text{HD}) - \delta(\text{H}_2)$ when both the H₂ and HD are trans to H or when they are both trans to D in the complexes **1Fe**, **2Fe**, and **1Ru**; there are small shifts (-20 and -50 ppb, respectively, for **2Ru**) (Table VII). However, there is a shift of 30–70 ppb when trans hydride is replaced by trans deuteride in these complexes. This shift, which is in the expected downfield direction, is another manifestation of the high trans influence of deuteride compared to hydride.⁵⁰ This phenomenon was also observed for the isotopomers of

Scheme III. Stereochemical Aspects of the Formation of Dihydrogen Complexes by Protonation of Dihydride Complexes

trans-[Os(H)(H₂)(*meso*-tetraphos-1)]⁺.¹² The isotopomers of **2Os** display similar isotopic shifts, but it must be noted that these chemical shift differences are temperature dependent.

Electrochemistry and Infrared Data. Complexes **1** and **2** are difficult to oxidize and display an anodic wave at $E_a \approx 1$ V vs FeCp₂/FeCp₂⁺ (Table VIII). The cathodic return wave is very broad and likely involves the reduction at the Pt electrode of protons produced in the oxidation reaction



The oxidation of the metal by **1** (adding **1** to the positive charge on the complex) is expected to decrease the pK_a of the coordinated dihydrogen ligand by about 20!⁵¹ In addition, the dihydrogen will become exceedingly labile in the oxidized complex, and thus loss of H₂ could also account for the irreversibility, at least for the Fe and Ru complexes. Removing one positive charge from **1** or **2** effectively gives a trihydride complex like **3Re**, which is easier to oxidize by about 1.4 V (Table VIII).

The infrared data for the corresponding carbonyl and dinitrogen complexes (Table VIII) reflect the electrochemical behavior of the $[MHL_2]^{n+}$ binding site in that the stretching frequencies for Re are much lower than those for complexes **1** and **2** as expected.⁵²

The complexes *trans*-M(Cl)(H)L₂ display more reversible redox behavior. These data suggest that the binding sites $[MHL_2]^+$ with M = Fe are more reducing than the Ru and Os complexes and those with L = *depe* are more reducing than those with L = *dppe*.

Discussion

Formation of Dihydrogen Complexes by Protonation. The fact that *cis* dihydride complexes lead to *trans* dihydrogen complexes in eq 1 provides some insight into the mechanism of formation of complexes **1** (Scheme III). The starting complexes of eq 1 have predominantly *cis* stereochemistry although RuH₂(*dppe*)₂ is ~5% *trans* according to ³¹P NMR and OsH₂(*dppe*)₂ is 10% *trans*.⁵³ The Fe complex is isomerizing at a rate of 150 s⁻¹ and

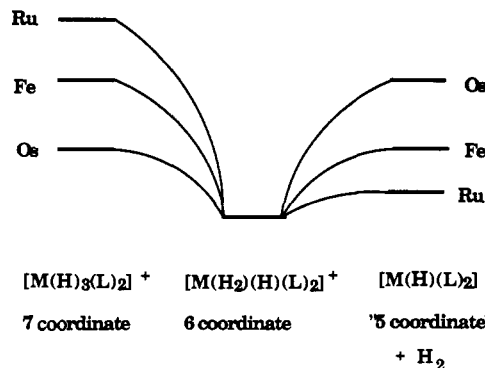


Figure 3. Qualitative energy level diagrams for (a) the seven-coordinate intermediates in the H atom exchange process of Scheme I and (b) the five-coordinate (or weakly solvated six-coordinate) complexes produced by the loss of H₂. The energy scales of the two sides of the diagram are not likely to be the same.

the Ru complex at a rate of <1 s⁻¹; the Os complex is essentially static.⁵⁴ The initial product of the very fast protonation of the *cis* complexes should be *cis*-[M(H)(*dppe*)₂(H₂)]⁺ (route 1, Scheme III) since there is mounting evidence that protonation of basic hydride complexes takes place at the hydride ligand;^{12,55-58} this might isomerize rapidly to its related trihydride form (route 2). Such *cis* intermediates must isomerize rapidly to the observed *trans* form; the *cis* form can only be stabilized by use of suitable tetraphos ligands as in [Fe(H)(PP₃)(H₂)]⁺^{14,59} and [OsH₃(*rac*-tetraphos-1)]⁺.¹² Attack at the metal between phosphorus atoms (route 3) would give the *trans* stereochemistry directly, but there is no evidence for the microscopic reverse of this process. For example, deprotonation of *trans*-[Ru(H)(*dppe*)₂(η^2 -H₂)]⁺ by BuLi at -80 °C gives thermally unstable *trans*-Ru(H)₂(*dppe*)₂ (Scheme III), which isomerizes to *cis*-Ru(H)₂(*dppe*)₂ at room temperature; the reverse of route 3 would lead to the incorrect *cis* stereochemistry.

A strong acid for eq 1 is not required. The dihydride complexes M(H)₂(*dppe*)₂ are completely protonated by 1 equiv of [Ru-(C₂H₅)(H)₂(PPh₃)₂]BF₄ ($pK_a \approx 8.3$) in THF⁵⁷ or by 1 equiv HPCy₃⁺BPh₄⁻ ($pK_a \approx 9.7$)⁶⁰ in THF.⁵¹ The complexes M(H)₂(*depe*)₂ (M = Fe,¹¹ Ru, and Os) are so basic that they dissolve in EtOH ($pK_a \approx 15.9$) and are completely converted to the dihydrogen complexes **2** (OEt⁻ counterion).⁵¹ This unexpected reactivity with alcohol explains why the dihydride complexes could not be made by the standard method of reaction of LiAlH₄ with the dichloride complexes followed by deactivation and decomplexation of the aluminum salts by addition of alcohol.⁶¹ Further investigation of the relative kinetic and thermodynamic acidities of complexes **1** and **2** is in progress.

Metal Dihydrogen Interaction. The qualitative rates of eq 3 and the H₂/D₂ exchange reactions give a sense of the relative strengths of the metal-dihydrogen interactions. Dihydrogen reacts rapidly with the five-coordinate complexes of all three metals generated by chloride removal as in eq 3. Five-coordinate complexes of this type are thought to have a square-pyramidal geometry^{34,62,63} although it is possible that a sixth ligand (a solvent molecule or a phosphine C-H bond) may also be weakly coor-

(53) Maltby, P. A. M.Sc. Thesis, University of Toronto, 1988.

(54) Meakin, P.; Muetterties, E. L.; Jesson, J. P. *J. Am. Chem. Soc.* **1973**, *95*, 75-88.

(55) Conroy-Lewis, F. M.; Simpson, S. J. *J. Chem. Soc., Chem. Commun.* **1987**, 1675-1676.

(56) Crabtree, R. H.; Lavin, M.; Bonneviot, L. *J. Am. Chem. Soc.* **1986**, *108*, 4032-4037.

(57) Jia, G.; Morris, R. H. *Inorg. Chem.* **1990**, *29*, 581-582.

(58) Parkin, G.; Bercaw, J. E. *J. Chem. Soc., Chem. Commun.* **1989**, 255-257.

(59) Bampos, N.; Field, L. D. *Inorg. Chem.* **1990**, *29*, 587-588.

(60) Bush, R. C.; Angelici, R. J. *Inorg. Chem.* **1988**, *27*, 681-686.

(61) Chatt, J.; Hayter, R. G. *J. Chem. Soc.* **1961**, 2605.

(62) Ashworth, T. V.; Singleton, E. *J. Chem. Soc., Chem. Commun.* **1976**, 705-706.

(63) Ashworth, T. V.; Chalmers, A. A.; Singleton, E. *Inorg. Chem.* **1985**, *24*, 2125-2126.

(51) Cappellani, E. P.; Drouin, S. M.; Jia, G.; Maltby, P. A.; Morris, R. H.; Schweitzer, C. T. Manuscript in preparation.

(52) Morris, R. H.; Earl, K. A.; Luck, R. L.; Lazarowich, N. J.; Sella, A. *Inorg. Chem.* **1987**, *26*, 2674-83.

dinated.² The lability of dihydrogen as judged by the qualitative H_2/D_2 rates of exchange increases as $Os < Fe < Ru$. Thus, the equilibrium constant for H_2 binding and hence the strength of the H_2 -metal bond likely increases as $Ru < Fe < Os$. Figure 3 qualitatively expresses the energetics of this equilibrium between five- and six-coordinate complexes. There is partial evidence that this ordering is valid in the solid state since **1Ru** is the only complex that reversibly loses and recoordinates H_2 gas in the solid state at 25 °C. The ordering of strength of the metal- H_2 interaction might be expected to parallel the magnitude of the coupling between the H_2 nuclei and ^{31}P nuclei in the complexes, $^2J(H_2,P)$; however, the uncertainties in this coupling only allow the conclusion that **2Os** has a stronger interaction with H_2 than the other complexes (Table II).

The ordering of H_2 lability is consistent with relative rates of substitution of the complexes; the complexes react irreversibly with CH_3CN to give complexes *trans*- $[M(H)(CH_3CN)(L)_2]^+$ with qualitative rates increasing as $Os \ll Fe \approx Ru$. A similar trend in lability of dihydrogen was noted for complexes containing monodentate phosphine ligands, $[M(H)(H_2)\{PPh(OEt)_2\}_4]^+$.⁵

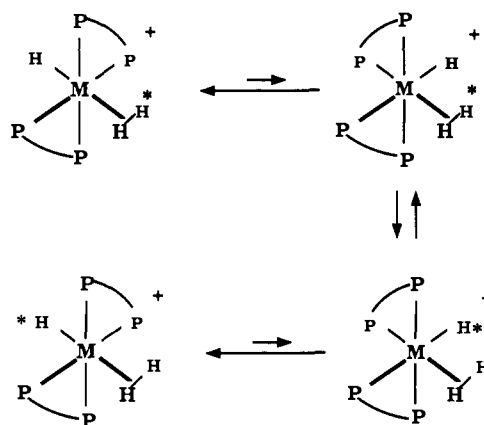
H-H Bonding. The T_1 and $^1J(H,D)$ measurements suggest an ordering of H-H bond length and strength. The H-H distances for the Fe and Ru complexes with rapidly spinning dihydrogen ligands are comparable at 0.87 ± 0.02 Å, considering the accuracy of the T_1 method, and are consistent with the value of 0.82 (2) for **1Fe** at 10 K as determined by neutron diffraction. This distance is apparently insensitive to the differences in the electronic properties of the metals (Ru versus Fe) and the ligands (dppe versus depe) as detected by electrochemistry. The Os complexes (**1Os**) and the dihydrogen tautomer of **2Os**) have significantly longer H-H bonds (~ 1.0 Å). Thus, an overall ordering of increasing distances is $Ru \approx Fe < Os$. There is a greater variation in $^1J(H,D)$ with regard to changes in metal and ligand in the complexes *trans*- $[M(D)(\eta^2-HD)L_2]^+$. If this coupling gives an indication of H-H (H-D) bond order, then H-H bond strength should decrease in the order **1Ru** \geq **2Ru** \geq **1Fe** $>$ **2Fe** $>$ **1Os** \approx **2Os**, although the actual coupling for the η^2-HD tautomer of **2Os** can only be estimated.²⁹

If it is assumed that the H-H bond order decreases as the metal- H_2 interaction increases, then this H-H bond order ranking is consistent with the metal- H_2 interaction given above. This is understood in terms of bonding arguments where H-H bond order decreases and the M-H bond order increases as σ -withdrawal of electrons from the $\sigma(H_2)$ orbital by the metal increases and π -donation from d_π orbitals into the $\sigma^*(H_2)$ orbital increases on going from Ru to Fe to Os and from less basic dppe complexes to more basic depe complexes. The π -back-bonding component to the bonding just mentioned is difficult to distinguish from an increase in σ -bonding to the separate H atoms since both processes involve orbitals of the same symmetry.

The simplest rationalization of the ordering down the triad is that π -back-bonding increases going from Ru(II) to Os(II) to Fe(II) and σ -bonding increases going from Fe to Ru to Os. Thus, Os would form the strongest M- H_2 bonds based on σ - and π -contributions, while Ru forms the weakest due to poor π -bonding. The increase in σ -bond strength down the triad is well-known,⁶⁴ and Os is expected to form the strongest σ -bonds because of improved overlap due to relativistic contraction of its orbitals.⁶⁵

The ordering of capacity for π -back-bonding as $Ru(II) < Os(II) < Fe(II)$ is more controversial. The results from cyclic voltammetry on the dihydrogen complexes do not provide a clear-cut ranking of electron richness because the redox behavior is irreversible. We propose that the $[FeH(depe)_2]^+$ unit is the best back-bonder since it forms the most reducing complexes (Table VIII) and has the CO and N_2 complexes with lowest stretching frequencies of the three metals. The corresponding Os complex should be more electron releasing than the Ru complex since it is slightly easier to oxidize (Table VIII) and back-bonds better to N_2 . However, a comparison of the stretching frequencies of

Scheme IV. Intramolecular Exchange Process That is Unlikely



CO complexes of Ru and Os (Table VIII) suggests that Ru is a better back-bonder than Os. Subtle changes in overlap and energetics of the d orbitals must account for this difference. In classical coordination complexes, Os almost always gives complexes that are more reducing than isostructural Ru ones.⁶⁶ Taube and co-workers have shown that pentaammine Os(II) complexes are better π -bases than corresponding Ru(II) ones.⁶⁷ It is also possible that the single radial node of the 4d orbital of Ru falls in the M-H bonding region and thus decreases both σ - and π -overlap with ligand orbitals. In a series of isostructural, zero-valent alkyne complexes, $M(CO)_4(\eta^2-Me_3SiC_2SiMe_3)$, the π -back-bonding to alkyne increases as $Fe(0) < Ru(0) < Os(0)$ but the Ru complex is the most labile.⁶⁸ Note, however, the difference in metal oxidation state, coordination geometry, and bonding, which involves 2p orbitals on C separated by 1.3 Å.

Intramolecular H Atom Exchange and the Homolytic Cleavage of H_2 . There are several possible mechanisms for the exchange process of Scheme I. As we reported earlier, homolytic cleavage of the H-H bond to give a fluxional trihydride intermediate, which allows H atom exchange, is most consistent with the data.^{25,29} Other possible mechanisms are considered below. The ΔG^\ddagger values decrease as $Ru > Fe > Os$ and $dppe > depe$. This ordering differs from those observed for classical hydride complexes $MH_2(PR_3)_4$ where the barriers were relatively insensitive to ligand variation but decreased as $Os > Ru > Fe$.⁶⁹ The ordering also differs from that of $MH_2(diphosphine)_2$ (Table IV) where the dmpe complex has a higher barrier than the dppe one. This is the opposite order to **1** and **2** considering that depe and dmpe have similar properties as ligands.⁵⁴ The small ΔS^\ddagger values are in accord with an intramolecular process.⁷⁰

Estimates of the rates of exchange between the two equivalent hydrides and the terminal hydride in the pentagonal bipyramidal trihydride $ReH_3(dppe)_2$ (**3Re**) (see Table IV, ref 29) were also examined. The ΔG^\ddagger value obtained for **3Re** fits well in the trend that, as the hydridic character of the dihydrogen ligand increases (**1Ru** \approx **1Fe** $<$ **1Os** $<$ **3Re**), the barrier to rearrangement decreases. This trend supports the existence of a fluxional trihydride intermediate in Scheme I. The ΔG^\ddagger value for the interconversion of $W(CO)_3(H_2)(P(i-Pr)_3)_2$ to $W(H)_2(CO)_3(P(i-Pr)_3)_2$ is 16.0 kcal mol⁻¹.⁷¹ The dihydride in this case is thought to have a capped octahedral geometry. The depe complexes have lower ΔG^\ddagger values than those of the dppe complexes. The more electron donating depe ligand would encourage the formation of the trihydride transition state more than the dppe ligand. Their smaller size

(66) Lever, A. B. P. *Inorg. Chem.* **1990**, *29*, 1271-1285.

(67) Lay, P. A.; Magnuson, R. H.; Taube, H. *Inorg. Chem.* **1988**, *27*, 2848-2853.

(68) Ball, R. G.; Burke, M. R.; Takats, J. *Organometallics* **1987**, *6*, 1918-1924.

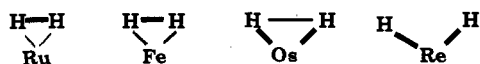
(69) Meakin, P.; Guggenberger, L. J.; Peet, W. G.; Muetterties, E. L.; Jesson, J. P. *J. Am. Chem. Soc.* **1973**, *95*, 1467-1474.

(70) A reviewer of this paper reports that there are some dissociative reactions with small ΔS^\ddagger values.

(71) Khalsa, G. R. K.; Kubas, G. J.; Unkefer, C. J.; van Der Sluis, L. S.; Kubat-Martin, K. A. *J. Am. Chem. Soc.* **1990**, *112*, 3855-3860.

(64) Tilset, M.; Parker, V. D. *J. Am. Chem. Soc.* **1989**, *111*, 6711-6717.

(65) Pyykkö, P. *Chem. Rev.* **1988**, *88*, 563-594.

Chart I. Qualitative H–H Interactions and M–H Interactions as Expressed by Light Lines (Weak, Long Bonds) and Heavy Lines (Strong, Short Bonds)

would also stabilize this intermediate. The ordering of stability of seven-coordinate trihydride intermediates in the exchange process of Scheme I is illustrated in Figure 3; note that Ru is out of the periodic order.

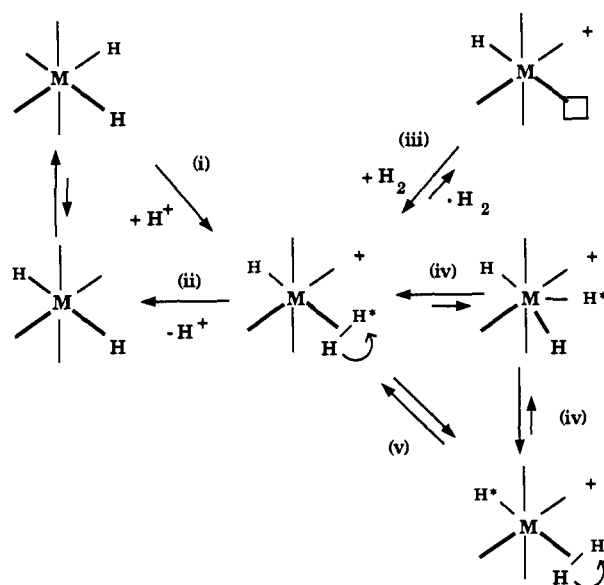
An alternative mechanism involving a rapid equilibrium before the rate-determining step of *trans* \rightleftharpoons *cis* isomerization of the octahedral complexes to bring the exchanging groups *cis* to each other (Scheme IV) can be probably discarded because the coupling constant ${}^2J(H,P)$ of the terminal hydride would be a weighted average of several *cis* $J(H,P)$ couplings with a *trans* $J(H,P)$ coupling constant to give values that would likely be temperature dependent and larger than the ones observed, at least for Ru and Os (Table II).⁷² Furthermore, for all the complexes **1** and **2** at temperatures where H atom exchange is slow on the NMR time scale, only the *trans* isomer is observed. In addition, the observed ordering of ΔG^\ddagger values (Ru > Fe > Os) is not consistent with a six-coordinate intermediate since six-coordinate dihydride complexes give the ordering Os > Ru > Fe (see above). Certainly when η^2-H_2 and H^- ligands are held *cis* to each other, as in $[Ir(C_{13}H_8N)(H)(H_2)(PPh_3)_2]^+$,⁵⁶ $[Re(H_2)(H)_2(CO)(PPh_3)_3]^+$,⁷³ or $[Fe(H)(H_2)(PP_3)]^+$,^{14,59} rapid intramolecular exchange can proceed by a formal deprotonation of the dihydrogen by the hydride base or by formation of a trihydrogen ligand (H_3).

Intermolecular acid–base reactions where the terminal hydride of another complex or the solvent accepts a proton from the H_2 ligand cannot explain the spectra. The rate of H atom exchange is unperturbed by the addition of excess HBF_4 . The ${}^2J(H,P)$ couplings are not lost during H atom exchange, which is not consistent with intermolecular exchange. The isotomers $[Os(HD)(H)L_2]^+$ and $[Os(HD)(D)L_2]^+$ of complexes **10s** and **20s** do not scramble H^+/D^+ by intermolecular exchange over a period of hours and hence do not give statistical mixtures of all possible deuterated species. Also the rate of proton transfer between complexes $[M(H)(dppe)_2(H_2)]^+$ and $M'H_2(dppe)_2$ is known to be much slower than H atom exchange.⁵¹

The rate-determining dissociation of one end of the diphosphine to give a six-coordinate trihydride intermediate, $[M(H)_3(P-P)(P-P)^*]^+$, where P^* is not coordinated, can also be discounted. The M–P bond energies increase as Fe–P < Ru–P < Os–P, which is not the ordering of activation energies. For the Fe complexes, which are the most likely to have labile phosphorus donors,⁷⁴ the bond strengths should increase as Fe(dppe) < Fe(depe), and this is not the order of ΔG^\ddagger values.

Conclusions

Chart I graphically represents the features of structure and bonding of the metal–dihydrogen unit in the complexes *trans*- $[M(HH)(H)(L)_2]^{n+}$ ($n = 0$ for Re; $n = 1$ for Fe, Ru, and Os) as deduced in this work. The Fe and Ru complexes have similar H–H distances in their rapidly spinning dihydrogen ligands. However, the Ru complexes have weaker interactions with the dihydrogen ligand than Fe (or Os). This difference is explained by the better back-bonding capability of the Fe center. The H–H distances in the Os complexes are significantly longer, and in the case of **20s** there are dihydrogen–hydride and trihydride tautomers present.³¹ The Os complexes have the strongest metal– H_2 bond of the triad because of the greater σ -bond energy than that of corresponding Fe complexes and greater σ - and π -energies than those of corresponding Ru complexes. The complex **3Re** is a trihydride because Re–H bonds are strong and the neutral ReH–

Scheme V. Chemical and Dynamic Processes of the Dihydrogen Complexes

(dppe)₂ unit is strongly electron releasing as indicated by the electrochemistry and infrared data.

The dihydrogen ligand undergoes a rich variety of chemical and dynamic processes as summarized in Scheme V: acid–base chemistry (routes i and ii), intermolecular loss/recoordination of H_2 (route iii), homolytic cleavage of H_2 leading to a trihydride tautomer (route iv) that leads to intramolecular H atom exchange (route v), and finally spinning of H_2 .

There is a continuous decrease in ${}^1J(H,D)$ (Table VII), in the lability of the dihydrogen, in the barrier to site exchange (Table IV), and in the chemical shifts difference, $\delta(\text{dihydrogen}) - \delta(\text{terminal hydride})$ (Table II), as one goes from **1Ru**, **2Ru** > **1Fe**, **2Fe** > **1Os** > **2Os** > **3Re**. The $T_{1\rho}(\text{min})$ values decrease in almost exactly the opposite order. Electrochemical and infrared data both indicate that the ease of oxidation of the binding sites for N_2 and Cl^- decreases as $ReH(dppe)_2 \gg [FeH(depe)_2]^+ > [FeH(dppe)_2]^+ > [MH(depe)_2]^+ > [MH(dppe)_2]^+$ ($M = Ru, Os$).

Thus, the Ru dihydrogen complexes have properties that are out of place in the periodic order. The $[RuHL_2]^+$ unit is a poorer π -back-bonder than the corresponding Fe complex because of its less energetic 4d electrons. Ru is a poorer σ -bonder and π -back-bonder than Os probably because the Os valence orbitals, due to relativistic contraction effects, have better overlap with ligand orbitals.

We propose that, for this series of iron group complexes, the energy difference between dihydrogen on an octahedral, d^6 center and dihydride on a seven-coordinate d^4 center is high for the Fe and Ru complexes but drops to a low value at Os where the metal center is sufficiently electron releasing (or σ -bonding becomes sufficiently strong) to give an elongated dihydrogen H–H distance of about 1.0 Å. Neutron diffraction will play a key role in determining the structure of such hydrides in this transition region.

Experimental Section

Unless otherwise noted, all manipulations were done in an Ar or H_2 atmosphere by use of Schlenk techniques. Solids were handled in a Vacuum Atmosphere drybox under N_2 . All solvents were dried over appropriate reagents⁷⁵ and distilled under N_2 before use. D_2 was obtained from Matheson Gas Products. Phosphines ligands were purchased from Strem Chemical Co. or Digital Specialty Chemicals Ltd. Literature methods were used to make $FeH_2(dppe)_2 \cdot 2C_2H_6$,⁷⁶ $FeH(C_6H_4PPhCH_2CH_2PPh_2)(dppe)$,⁷⁷ $[FeH(dppe)_2]BPh_4$,⁷⁸ $FeCl_2(depe)_2$,⁷⁹

(72) However, the *cis* intermediate might be present in such a small concentration that its contribution to the averaged coupling would be undetectable.

(73) Luo, X.-L.; Crabtree, R. H. *J. Am. Chem. Soc.* **1990**, *112*, 6912–6918.

(74) Henderson, R. A. *J. Chem. Soc., Dalton Trans.* **1988**, 515–520.

(75) Perrin, D. D.; Armarego, W. L. F.; Perrin, D. R. *Purification of Laboratory Chemicals*; Pergamon: Toronto, 1980.

(76) Peet, W. G.; Gerlach, D. H. *Inorg. Synth.* **1974**, *15*, 38.

(77) Azizian, H.; Morris, R. H. *Inorg. Chem.* **1983**, *22*, 6–9.

(78) Giannoccaro, P.; Sacco, A.; Ittel, S. D.; Cushing, J., M. A. *Inorg. Synth.* **1977**, *17*, 69.

$\text{FeHCl}(\text{depe})_2$,⁸⁰ and $\text{Ru}(\text{cod})(\text{cot})$.⁸¹ An improved synthesis of $\text{RuH}_2(\text{dppe})_2$ ⁸¹ in two steps from $\text{RuCl}_2(\text{DMSO})_4$ ⁸² is given below. The osmium complexes were prepared as described previously.^{29,61} Infrared spectra were recorded with use of a Nicolet 5DX FTIR spectrometer as Nujol mulls on NaCl plates or in the stated solvent in 0.1 mm KBr solution cells. NMR spectra were obtained on a Varian XL-400 operating at 400.00 MHz for ¹H and 161.98 MHz for ³¹P or on a Varian XL-200 operating at 200.00 MHz for ¹H and 80.98 MHz for ³¹P. Some variable-temperature ³¹P NMR and selective hydride decoupling experiments were carried out by use of the Bruker WP400 spectrometer at the South Western Ontario Regional NMR facility. Chemical shifts refer to room temperature conditions unless specified otherwise. All ³¹P NMR were proton decoupled. ³¹P chemical shifts were measured relative to ~1% P(OMe)₃ in C₆D₆ sealed in coaxial capillaries but are reported in parts per million from 85% H₃PO₄ ($\delta(\text{P}(\text{OMe})_3) = 140.4$ ppm). ¹H chemical shifts (ppm) were measured relative to partially deuterated solvent peaks but are reported relative to tetramethylsilane. *T*₁ measurements were made by using the inversion recovery method.¹³ Care was taken in the preparation of the complexes to avoid paramagnetic species like $[\text{FeH}(\text{depe})_2]^+$, which would contribute to the overall rate of relaxation. Dynamic NMR spectra were simulated with use of a modified version of the program DNMR4,⁸³ and second-order spectra were simulated with use of the LAOCN 5 program.⁸⁴

Microanalyses were performed by the Canadian Microanalytical Service, Ltd., Westminster, B.C. A PAR Model 273 potentiostat was used for cyclic voltammetry studies. The electrochemical cell contained a Pt working electrode, W secondary electrode, and Ag wire reference electrode in a Luggin-Haber probe-type capillary; THF or CH₂Cl₂ solutions were 0.002 M in the complexes and 0.2 M in *n*-Bu₄NBF₄. Reported potentials are referenced to ferrocene, which was added to these solutions.

Preparation of *trans*-[FeH(dppe)₂(η²-H₂)]BF₄ (1Fe). Dinitrogen as well as dioxygen must be excluded at all stages by use of a H₂ or Ar atmosphere. Method 1: FeH₂(dppe)₂·2C₇H₈ (0.5 g, 0.58 mmol) was partially dissolved in 50 mL of diethyl ether to produce a yellow suspension. Under 1 atm of argon or hydrogen, 0.5 mL of HBF₄·Et₂O (excess) was added dropwise over a period of 1 min with stirring. Immediately a pale yellow, powdery solid precipitated out, causing the solution to turn almost colorless. The solid was filtered off and washed several times with diethyl ether (80% yield). The product can be recrystallized by slow diffusion of diethyl ether into a THF solution of 1Fe and washed with cold THF, MeOH, and diethyl ether. The product contains THF and ether in the lattice as verified by X-ray diffraction. Anal. Calcd for C₃₂H₃₁BF₄FeP₄(C₆H₈O)₂(C₄H₁₀O): C, 66.22; H, 6.7. Found: C, 66.27; H, 6.0. IR (Nujol): 1919 (Fe-H), 1050 cm⁻¹ (BF₄⁻). UV-vis: λ_{max} 380 nm (ε 255). ¹H NMR: see Figure 1. Method 2: When HBF₄·Et₂O (35 μL, 0.25 mmol) was added to a solution of FeH(C₆H₅PPhCH₂CH₂PPh₂)(dppe) (200 mg, 0.23 mmol) in toluene at -5 °C under H₂, a purple precipitate ([FeH(dppe)₂]BF₄, see ref 78) formed immediately but then turned to a light yellow solid (1Fe) within 1 min.

Preparation of *trans*-[Fe(H)(dppe)₂(η²-H₂)]BPh₄ (1FeBPh₄) from FeClH(dppe). FeClH(dppe)₂ (0.064 g, 0.072 mmol) was dissolved in 15 mL of a THF/EtOH mixture (50% by volume) to form a deep purple solution. To this solution was added a solution of NaBPh₄ (0.026 g, 0.076 mmol) in 5 mL of EtOH under H₂. Within 10 min, the deep purple color of the solution had lightened to pink, and after it was stirred for 12 h the solution was cloudy yellow. The yellow solid (0.053 g, 0.045 mmol), isolated by filtration, was washed with benzene, water, and diethyl ether to give 1FeBPh₄ in 62% yield, which is spectroscopically pure (¹H, ³¹P, cyclic voltammetry).

Preparation of *cis*-RuCl₂(dppe)₂. RuCl₂(DMSO)₄ (0.500 g, 1.00 mmol) was dissolved in 7 mL of CH₂Cl₂. Dppe (0.830 g, 2.10 mmol) in 5 mL of CH₂Cl₂ was added, and this clear yellow solution was stirred

for 1 h. After this time, the solvent was removed and the resulting yellow solid was washed with hexanes. The solid was then vacuum dried and recrystallized from THF/hexane. The product contained a mixture of *cis*/*trans* isomers in an approximate ratio of 3:1, and further recrystallization was therefore necessary to eliminate the unreactive *trans* isomer (δ 43.6 in ³¹P NMR spectrum). This was achieved by making a concentrated solution in CH₂Cl₂ and carefully placing a layer of hexanes above this. Upon cooling, the pure *cis* isomer crystallized out in 60% yield. ³¹P NMR (81 MHz, CD₂Cl₂): 49.9 (t), 36.9 (t, *cis* isomer, ²*J*_{PP} = 19.7 Hz).

***cis*- and *trans*-RuCl₂(depe)₂** was prepared in a similar manner in 71% yield. ³¹P NMR (81 MHz, C₆D₆, *cis*/*trans* ~8): 47.7 (s, *trans* isomer), 59.0 (t), 47.4 (t, *cis* isomer, ²*J*_{PP} = 22.4 Hz).

Preparation of *cis*-RuH₂(dppe)₂. *cis*-RuCl₂(dppe)₂ (0.500 g, 0.51 mmol) was dissolved in a mixture of THF (8 mL) and EtOH (2 mL). Under 1 atm of H₂ or Ar, 0.140 g of NaOEt (2.00 mmol) was added with stirring. This yellow solution was stirred for 15 h. After this time, the solution slightly discolored to pale yellow. The solvent was removed, and the solid was redissolved in benzene. The NaCl formed was filtered off through Celite, and the volume of the filtrate was reduced to 2 mL. Addition of hexane caused precipitation of the cream-colored RuH₂(dppe)₂ in 60% yield (0.277 g). ¹H NMR (200 MHz, C₆D₆, *cis*/*trans* ~20): -8.17 (q, *J*_{HH} ≈ 17 Hz, *trans*-RuH₂), -8.33 (AA' part of AA'MM'X₂ pattern, *J*_{AA'} = -1 or -4, *J*_{MM'} = -4 or -1, *J*_{AM} = *J*_{AM'} = 68, *J*_{AM}' = *J*_{AM} = -15.2, *J*_{AX} = *J*_{AX}' = -23.5 Hz, *cis*-H₂Ru). ³¹P NMR (81 MHz, C₆D₆, *cis*/*trans* ~20): 83.4 (s, *trans*-H₂Ru), 79.0 (X₂ part of MM'X₂ pattern, ²*J*_{MX} ≈ 15.5 Hz), 65.0 (MM' part of MM'X₂ pattern).

Preparation of *trans*-[RuH(dppe)₂(η²-H₂)]BF₄ (1Ru) from RuH₂(dppe)₂. Method 1 for the preparation of 1Fe was followed except that RuH₂(dppe)₂ was used. All solutions were kept under 1 atm of dihydrogen, and the solid product was dried in a stream of dihydrogen. IR (Nujol): 1961 (Ru-H), 1050 cm⁻¹ (BF₄⁻). ¹H NMR: see Figure 2.

Preparation of *trans*-[RuH(dppe)₂(η²-H₂)]BPh₄ (1RuBPh₄) from RuCl₂(dppe)₂. A mixture of *cis*- and *trans*-RuCl₂(dppe)₂ (0.500 g, 0.51 mmol) was dissolved in 10 mL of THF. Under 1 atm of H₂, NaBPh₄ (0.700 g, 2.0 mmol) was added with stirring; immediately the cloudy yellow mixture changed to orange and after approximately 0.5 min discolored back to yellow. This mixture was stirred for 3.5 h after which time it was filtered through Celite and the filtrate removed under reduced pressure. Under 1 atm of H₂, the residue was dissolved in a minimum of acetone. Addition of MeOH resulted in the precipitation of a cream solid (0.288 g, 46%), which was washed with MeOH and dried under a stream of dihydrogen. Anal. Calcd for C₇₆H₆₉BP₄Ru (sample that lost H₂): C, 74.94; H, 5.71. Found: C, 74.59; H, 5.77.

Observation of *trans*-RuH₂(dppe)₂ by Reaction of 1RuBPh₄ with BuLi. A solution of 1Ru (0.026 g, 0.021 mmol) in 2 mL of acetone-*d*₆ was cooled to 200 K under 1 atm of H₂. BuLi in hexane (0.014 mL of 1.6 M) was then added by syringe, and the solution was stirred at 200 K under H₂ for 2 h. The ¹H NMR spectrum in the hydride region showed only a broad quintet for the product at -8.62 ppm (²*J*(H,P) = 18 Hz). When this solution warmed to room temperature, the only hydride resonance present was the multiplet due to *cis*-RuH₂(dppe)₂ at -8.75 ppm. The resonances for a small amount of the *trans* isomer could be hidden under this multiplet.

Preparation of *trans*-[Fe(H)(depe)₂(η²-H₂)]BPh₄ (2Fe) from FeClH(depe). FeClH(depe)₂ (0.28 g, 0.56 mmol) was dissolved in 25 mL of acetone. Under 1 atm of H₂, NaBPh₄ (0.24 g, 0.7 mmol) was added and the mixture was stirred for 30 min. The resulting NaCl was filtered off through Celite, and the volume of the filtrate was reduced to 5 mL. MeOH (5 mL) was added, and the solution was cooled overnight to give yellow-orange crystals of 2Fe (0.12 g, 0.168 mmol) in 30% yield, which were washed with cold MeOH and diethyl ether. Anal. Calcd for C₄₄H₇₁BF₄FeP₄·CH₃OH: C, 65.70; H, 9.19. Found: C, 65.80; H, 8.86.

Preparation of *trans*-[Fe(H)(depe)₂(η²-H₂)]BPh₄ (2Fe) Directly from FeCl₂(depe)₂. Sodium ethoxide/EtOH solution (0.25 mL, 0.217 M) was added via syringe to a solution of NaBPh₄ (0.0187 g, 0.055 mmol) in 15 mL of EtOH. The solution was cooled to 14 °C, FeCl₂(depe)₂ (0.0291 g, 0.054 mmol) was added, and the mixture was placed under H₂. The color changed from light green to yellow initially; over the course of 5 min, the solution became clear and the white product precipitated out. Hydrogen uptake was measured to be 1.7 mol of H₂/Fe over the course of this reaction. The solid was collected by filtration and washed with EtOH, water, and finally diethyl ether. It was pure according to spectroscopic and electrochemical methods.

Preparation of *cis*- and *trans*-RuH₂(depe)₂. Ru(cod)(cot) (0.300 g, 0.95 mmol) was dissolved in THF (8 mL). Under 1 atm of hydrogen, depe (0.395 g, 1.9 mmol) was added dropwise. This bright yellow solution was stirred for 24 h after which time it had discolored to a pale yellow. The solvent was removed under reduced pressure. Under 1 atm

(79) Baker, M. V.; Field, L. D.; Hambley, T. W. *Inorg. Chem.* **1988**, *27*, 2872-2876.

(80) Chatt, J.; Hayter, R. G. *J. Chem. Soc.* **1961**, 5507.

(81) Pertici, P.; Vitulli, G.; Poarzio, W.; Zocchi, M. *Inorg. Chim. Acta Lett.* **1979**, *37*, L521.

(82) Chaudret, B.; Commenges, G.; Poilblanc, R. *J. Chem. Soc., Dalton Trans.* **1984**, 1635-1639.

(83) Bushweller, C. H.; Letenare, L. J.; Brunelle, J. A.; Bilofsky, H. S.; Whalon, M. R.; Fleischman, S. H. *Quantum Chemistry Program Exchange*, No. 466, DNMR-4.

(84) Cassidei, L.; Sciacovelli, O. *Quantum Chemistry Program Exchange*, No. 458, LAOCN 5.

(85) Smith, G.; Cole-Hamilton, D. J. *J. Chem. Soc., Dalton Trans.* **1984**, 1203-1208.

(86) Moehring, G. A.; Walton, R. A. *J. Chem. Soc., Dalton Trans.* **1987**, 715-720.

(87) Bradley, M. G.; Roberts, D. A.; Geoffroy, G. L. *J. Am. Chem. Soc.* **1981**, *103*, 379-384.

of Ar, cold acetone was added to the residue, affording a white solid (0.080 g, 16%). ^1H NMR (200 MHz, C_6D_6 , cis/trans \sim 2: -10.24 (q, $^2J(\text{H,P}) = 22.4$ Hz, *trans*- H_2Ru), -10.64 (AA' part of AA'MM'X₂ pattern, $J_{\text{AA}'} = -24$ or 0, $J_{\text{MM}'} = 0$ or -24, $J_{\text{AM}} = J_{\text{AM}'} = 60$, $J_{\text{AM}'} = J_{\text{AM}} = -12$, $J_{\text{AX}} = J_{\text{AX}'} = -24$ Hz, *cis*- H_2Ru). ^{31}P NMR (81 MHz, THF, cis/trans \sim 2): 84.3 (s, *trans*- H_2Ru), 76.0 (X₂ part of MM'X₂ pattern, $J_{\text{MX}} = J_{\text{MX}'} = -22.4$ Hz, *cis*- H_2Ru), 62.7 (MM' part of MM'X₂ pattern, *cis*- H_2Ru).

Preparation of *trans*-[Ru(H)(depe)₂(η^2 -H₂)]BPh₄ (2Ru). RuHCl(depe)₂ (0.185 g, 0.33 mmol) was dissolved in acetone (5 mL). Under 1 atm of hydrogen, NaBPh₄ (0.173 g, 0.50 mmol) was added with stirring. This yellow solution was stirred overnight after which time it was filtered through Celite under an argon atmosphere. The volume of the filtrate was reduced to 2 mL. Addition of methanol caused the precipitation of a white solid, which was washed with MeOH and dried in vacuo (0.190 g, 68%). Anal. Calcd for C₄₄H₇₁BP₄Ru: C, 63.22; H, 8.56. Found: C, 63.06; H, 8.45.

Preparation of *trans*-[Ru(H)(depe)₂(η^2 -H₂)]BPh₄ (2Ru) Directly from RuCl₂(depe)₂. RuCl₂(depe)₂ (0.030 g, 0.051 mmol) was dissolved in 3 mL of THF and 1 mL of ethanol. Under 1 atm of H₂, NaBPh₄ (0.018 g, 0.051 mmol) and NaOEt (0.007 g, 0.103 mmol) were added with stirring. This mixture was stirred for 1 h and then filtered through Celite under an atmosphere of argon. The solvent was removed under reduced pressure, and under an atmosphere of hydrogen the yellow-white residue was redissolved in a minimum of acetone. Addition of methanol caused the precipitation of the white product (0.020 g, 46%); unreacted *trans*-RuCl₂(depe)₂ remained dissolved in the methanol.

Preparation of *trans*-[Ru(η^2 -H₂)(H)(depe)₂](BF₄) (2RuBF₄). RuH₂(depe)₂ (0.050 g, 0.10 mmol) was dissolved in diethyl ether (20 mL). Under 1 atm of hydrogen, 0.1 mL of HBF₄·Et₂O (excess) was added dropwise with stirring. A white solid immediately precipitated. This white solid was allowed to settle, and the ether supernatant was syringed out. The solid (0.042 g, 72%) was then washed with diethyl ether (2 \times 5 mL) and cold MeOH (5 mL) to remove any excess acid and dried in vacuo.

Preparation of FeD₂(dppe)₂. FeCl₂ (9 mg, 0.07 mmol) was added to the dppe (64 mg, 0.16 mmol) in THF (25 mL) and stirred for 5 min, producing a tan-colored solution. NaBD₄ (9 mg, 0.24 mmol) in EtOD (4 mL) was added to the stirring solution. The solution was stirred for 12 h at 20 °C in darkness. After the boron-containing salts and excess FeCl₂ were filtered off, the volume of the yellow filtrate was reduced to approximately 3 mL and then 3 mL of diethyl ether and 7 mL of hexane were added to give the product (36 mg, 60%).

Preparation of 1Fe-*d*₂. FeD₂(dppe)₂ (35 mg, 0.042 mmol) was dissolved in diethyl ether. Under 1 atm of argon, HBF₄·Et₂O (0.20 mL, excess) was added over a period of 1 min with stirring. The resulting pale yellow precipitate (20 mg) was filtered and washed with diethyl ether. The ^1H NMR sample in acetone-*d*₆ was placed under 1 atm of D₂ for 45 min. In the hydride region of the ^1H NMR spectrum at 213 K, there

was a 1:1:1 triplet at -8.8 ppm and a quintet at -13.2 ppm. In similar experiments in CD₂Cl₂, the 1:1:1 triplet for 1Fe-*d*₁ was also partially resolved.

Observation of Isotopomers of 1Ru and 2Ru. Acetone-*d*₆ solutions of 1Ru or 2Ru were placed under 1 atm of HD (made by adding NaH to D₂O) for 5 min. The ^1H NMR spectra were recorded after every 15 min. H/D exchange with the acetone-*d*₆ resulted in progressive enrichment of the complexes in D so that first the *d*₁ and then the *d*₂ species were observed. The mixtures were also examined by D NMR.

Preparation of 1Fe-*d*₁. FeH₂(dppe)₂ (0.066 g, 0.07 mmol) was added to 10 mL of Et₂O containing 0.1 mL of D₂O. Approximately 0.05 mL of HBF₄·Et₂O was then added to produce DBF₄ in situ. The white precipitate was filtered and washed with three 5-mL volumes of Et₂O.

Preparation of Isotopomers 2-*d*₁. These complexes were synthesized from HD, NaBPh₄, and *trans*-MClH(depe)₂ as described above. The HD was generated by adding NaH to D₂O.

Preparation of Isotopomers 2-*d*₂. These complexes were synthesized from D₂, NaBPh₄, and *trans*-MClH(depe)₂ as described above. Os-*d*₂ was obtained in 50% yield.

Deuterium-Exchange Experiments. An NMR tube containing a solution of a complex (2) (27 mg, 0.03 mmol) and 10 μL of C₆D₆ was put under D₂ (1 atm) by bubbling D₂ through the solution for two min at 20 °C. The tube was shaken to overcome gas diffusion problems. After 1 h, Ar was bubbled through the solution to displace the D₂. D NMR showed incorporation of D by the appearance of a deuteride peak(s), which corresponded with the hydride patterns of complexes 2. There was no incorporation of D into the phosphine ligands. Integration of the deuteride peak(s) against the C₆D₆ peak allowed the calculation of a "half-life" or the time required for half the hydride and molecular hydrogen protons to be replaced by D atoms. Integration of the hydride resonances in the ^1H NMR as a function of time of exposure to D₂ against that of added silicone grease, which served as a standard, also gave a measure of the half-life.

To determine whether the rate of H₂/D₂ exchange was dependent on the pressure of D₂, the ^1H NMR spectra of three samples of 2Fe in acetone-*d*₆ containing initial partial pressures of deuterium mixed with argon of 0, 0.5, and 1.0 atm were recorded. Again, the disappearance of the hydride resonance was monitored by integrating it with respect to silicon grease. There was no noticeable pressure dependence.

Acknowledgment. This work was supported by grants to R. H.M. from NSERC Canada and the donors of the Petroleum Research Fund, administered by the American Chemical Society, and a loan of Ru and Os chlorides from Johnson Matthey Ltd. We thank Drs. Leslie Field, Robert Crabtree, and Clive Holloway and the reviewers for useful suggestions and Dr. Chris Pickett for advice and equipment concerning the electrochemical measurements.